

Impact of Crystalline Silicotitanate Particle Size on Cesium Removal Efficiency

October 2019

SK Fiskum
AM Rovira
MG Cantaloub
AM Carney
HA Colburn
RA Peterson
BD Pierson

DISCLAIMER

This report was prepared as an account of work sponsored by an agency of the United States Government. Neither the United States Government nor any agency thereof, nor Battelle Memorial Institute, nor any of their employees, makes **any warranty, express or implied, or assumes any legal liability or responsibility for the accuracy, completeness, or usefulness of any information, apparatus, product, or process disclosed, or represents that its use would not infringe privately owned rights**. Reference herein to any specific commercial product, process, or service by trade name, trademark, manufacturer, or otherwise does not necessarily constitute or imply its endorsement, recommendation, or favoring by the United States Government or any agency thereof, or Battelle Memorial Institute. The views and opinions of authors expressed herein do not necessarily state or reflect those of the United States Government or any agency thereof.

PACIFIC NORTHWEST NATIONAL LABORATORY
operated by
BATTELLE
for the
UNITED STATES DEPARTMENT OF ENERGY
under Contract DE-AC05-76RL01830

Printed in the United States of America

Available to DOE and DOE contractors from the
Office of Scientific and Technical Information,
P.O. Box 62, Oak Ridge, TN 37831-0062;
ph: (865) 576-8401
fax: (865) 576-5728
email: reports@adonis.osti.gov

Available to the public from the National Technical Information Service
5301 Shawnee Rd., Alexandria, VA 22312
ph: (800) 553-NTIS (6847)
email: orders@ntis.gov <<https://www.ntis.gov/about>>
Online ordering: <http://www.ntis.gov>

Impact of Crystalline Silicotitanate Particle Size on Cesium Removal Efficiency

October 2019

SK Fiskum
AM Rovira
MG Cantaloub
AM Carney
HA Colburn
RA Peterson
BD Pierson

Prepared for
the U.S. Department of Energy
under Contract DE-AC05-76RL01830

Pacific Northwest National Laboratory
Richland, Washington 99354

Summary

Washington River Protection Solutions is working on a Tank-Side Cesium Removal (TSCR) system to remove Cs from Hanford tank waste supernate. Removal of ^{137}Cs from tank waste supernate by TSCR results in a low-activity waste (LAW) form that can be fed directly to the Hanford Waste Treatment and Immobilization Plant (WTP) LAW vitrification facility, where the supernate can be vitrified into a glass form. Crystalline silicotitanate (CST) ion exchange media, manufactured by Honeywell UOP, LLC (product IONSIV™ R9140-B), was selected for use as the ion exchange media to remove Cs at TSCR.

The particle size used in testing is expected to impact the kinetic performance of the ion exchange media. Therefore, two single-column systems were tested with CST Lot 2002009604. One column contained <25 mesh sieve cut fraction and the other column contained <35 mesh sieve cut fraction. Flowrate through both test systems was adjusted to match the CST contact time expected for the full-scale operation, i.e., matched bed volumes per hour (BV/h) at 1.83 BV/h. The feed was processed downflow through the columns until ~1000 BVs of feed were processed.

The waste acceptance criteria (WAC) limit for the WTP LAW vitrification facility is $<3.18\text{E-}5 \text{ Ci } ^{137}\text{Cs}$ per mole Na.¹ For a tank waste containing $156 \mu\text{Ci/mL } ^{137}\text{Cs}$ and 5.6 M Na, up to 0.114% of the influent ^{137}Cs concentration may be delivered to the WTP (based on ^{137}Cs content in AP-107 tank waste);² this required a Cs decontamination factor of 876. The WAC limit was used as one of the relevant process parameters, along with the 50% breakthrough point, Cs loading per gram of CST, and the mass transfer zone.

Table S.1 summarizes the observed column performance determined for the two sieve fractions juxtaposed to the previous work with 5.6 M Na simulant at higher scales (used as benchmarks).³ The 50% Cs breakthroughs were nominally equivalent for all column tests.

- The smaller particle size (<35 mesh) CST resulted in 45-BV delay to the WAC limit and ~60-BV narrowing of the mass transfer zone. These improved performance characteristics were logical expectations from the available higher surface area available for Cs exchange and the concomitant shorter diffusion lengths into the CST beads.
- The <25 mesh CST resulted in reaching the WAC limit earlier (55 BVs) and slightly longer mass transfer zone (~50 BVs). The earlier Cs breakthrough was attributed to the slow superficial velocity negatively affecting film mass transfer.

Neither sieve cut Cs removal performances at the 10-mL CST bed geometry perfectly matched those of the 12% height and full height columns. It is recommended that an intermediate <30 mesh sieve cut be tested to determine if it better reflects the 12% and full height column performances at the 10-mL scale. The ultimate goal is to use the most appropriate sieve cut CST in future actual tank waste ion exchange column studies at the small-scale to improve the ability to predict full-scale behavior.

¹ From *ICD 30 – Interface Control Document for Direct LAW Feed*, 24590-WTP-ICD-MG-01-030, Rev. 1, 2017, Bechtel National, Inc. (River Protection Project Waste Treatment Plant), Richland, Washington.

² Rovira AM, SK Fiskum, HA Colburn, JR Allred, MR Smoot, and RA Peterson. 2018. *Cesium Ion Exchange Testing Using Crystalline Silicotitanate with Hanford Tank Waste 241-AP-107*. PNNL-27706, RPT-DFTP-011, Rev. 0, Pacific Northwest National Laboratory, Richland, Washington.

³ Fiskum SK, AM Rovira, JR Allred, HA Colburn, MR Smoot, AM Carney, TT Trang-Le, MG Cantaloube, EC Buck, and RA Peterson. 2019b. *Cesium Removal from Tank Waste Simulants Using Crystalline Silicotitanate at 12% and 100% TSCR Bed Heights*. PNNL-28527, Rev. 0; RPT-TCT-001, Rev. 0, Pacific Northwest National Laboratory, Richland, Washington.

Table S.1. Column Performance Summary with CST Lot 2002009604

Column Test	d_{50} Particle Size (μm) ^(a)	WAC Limit Breakthrough (BVs)	Maximum Test Cs Breakthrough (% C/C ₀)	Extrapolated 50% Cs Breakthrough (BVs)	Mass Transfer Zone 5% to 95% (BVs)
2.5% height <25 mesh	593	185	49.1	997	1094
2.5% height <35 mesh	479	285	46.4	1018	972
12% height, <25 mesh ^(b)	567	240	47.3	992 ^(c)	1044 ^(c)
Full height, unsieved ^(b)	633	240	36.5	1002 ^(c)	1020 ^(c)

(a) Cumulative particle undersize fraction, volume basis.

(b) Fiskum SK, AM Rovira, JR Allred, HA Colburn, MR Smoot, AM Carney, TT Trang-Le, MG Cantaloub, EC Buck, and RA Peterson. 2019. *Cesium Removal from Tank Waste Simulants Using Crystalline Silicotitanate at 12% and 100% TSCR Bed Heights*. PNNL-28527, Rev. 0; RPT-TCT-001, Rev. 0, Pacific Northwest National Laboratory, Richland, Washington.

(c) Recalculated as described in this report.

Acknowledgments

The authors thank the Analytical Support Operations (ASO) count room staff Mike Cantaloub and Truc Trang-Le for rapid ^{137}Cs tracer analysis of the column load samples. We thank Carolyn Burns for particle size analysis of the two sieve fractions of crystalline silicotitanate. We thank Renee Russell for conducting the technical reviews of the calculation files, test data packages, and this technical report. We also thank Matt Wilburn for technical editing of this report and Bill Dey for the quality reviews of the calculation packages and this report.

Acronyms and Abbreviations

ASO	Analytical Support Operations
AV	apparatus volume
BV	bed volume
CST	crystalline silicotitanate
DF	decontamination factor
DI	deionized
FD	feed displacement
FIO	for information only
GEA	gamma energy analysis
HV	high-voltage input
ID	internal diameter
LAW	low-activity waste
MCA	multichannel analyzer
PC	personal computer
PMT	photomultiplier tube
PNNL	Pacific Northwest National Laboratory
PSA	particle size analysis
PSD	particle size distribution
QA	quality assurance
R&D	research and development
ROI	region of interest
SV	system volume
TSCR	Tank-Side Cesium Removal
WAC	waste acceptance criteria
WRPS	Washington River Protection Solutions
WTP	Hanford Waste Treatment and Immobilization Plant
WWFTP	WRPS Waste Form Testing Program

Contents

Summary	iii
Acknowledgments.....	v
Acronyms and Abbreviations	vi
Contents	vii
1.0 Introduction.....	1.1
2.0 Quality Assurance.....	2.1
3.0 Test Conditions	3.1
3.1 CST Media.....	3.1
3.2 5.6 M Na Simulant.....	3.2
3.3 Ion Exchange Process Testing	3.3
3.3.1 Processing Conditions	3.7
3.4 Analysis	3.10
4.0 Column Processing Results.....	4.1
4.1 Cs Loading, Feed Displacement, and Water Rinse.....	4.1
4.2 On-line Detection Assessment.....	4.4
4.3 Cs Load Performance Comparisons.....	4.5
4.4 WAC Limit	4.8
4.5 Cs Load Capacity.....	4.9
4.6 Mass Transfer Zone	4.10
5.0 Conclusions.....	5.1
6.0 References.....	6.1
Appendix A – Column Load Data	A.1
Appendix B – Particle Size Analysis	B.1
Appendix C – On-line Gamma Analysis	C.1

Figures

Figure 3.1. Ion Exchange System Schematic <35 mesh CST (Color Code Green).....	3.4
Figure 3.2. Ion Exchange System Schematic <25 mesh CST with Inline Gamma Detection (Color Code Purple).....	3.4
Figure 3.3. Photograph of Ion Exchange System, <35-mesh CST, Color Code Green	3.5
Figure 3.4. Photograph of Ion Exchange System, <25-mesh CST, Color Code Purple	3.6
Figure 3.5. <35 Mesh (Green) Flowrate as a Function of Process Time	3.9
Figure 3.6. <25 Mesh (Purple) Flowrate as a Function of Process Time.....	3.9
Figure 4.1. <35 Mesh CST with 5.6 M Na Simulant at 1.83 BV/h, a) Linear-Linear Plot, b) Probability-Log Plot	4.2
Figure 4.2. <25 Mesh CST with 5.6 M Na Simulant at 1.83 BV/h, a) Linear-Linear Plot, b) Probability-Log Plot	4.3
Figure 4.3. Extrapolated to 50% Breakthrough, a) <35 mesh CST, b) <25 mesh CST	4.4
Figure 4.4. Cs Load Profile Comparisons, CST Lot 2002009604, 5.6 M Na Simulant	4.5
Figure 4.5. Comparison of Small-Scale Column Performance with <25 mesh CST and 5.6 M Na Simulant, AP-107, and AW-102, a) Linear-Linear Plot, b) Probability-Log Plot.....	4.7
Figure 4.6. System Volume to WAC Limit vs. Flowrate.....	4.9

Tables

Table 3.1. Physical Properties of Washed R9140-B CST Lot 2002009604	3.2
Table 3.2. 5.6 M Sodium Simulant Target Composition (Fiskum et al. 2019b).....	3.3
Table 3.3. Experimental Conditions for <35 Mesh CST (Green) Processing, August 5 to August 28, 2019.....	3.8
Table 3.4. Experimental Conditions for <25 Mesh CST (Purple) Processing, August 5 to August 28, 2019.....	3.8
Table 4.1. Comparison of BV to WAC Limit, 5.6 M Na Simulant	4.8
Table 4.2. Comparison of Cs Loading onto CST, 5.6 M Na Simulant	4.10
Table 4.3. Mass Transfer Zone Comparison, CST Lot 2002009604, 1.83 BV/h, 5.6 M Na Simulant.....	4.11

1.0 Introduction

The U.S. Department of Energy is working to expedite processing of Hanford tank waste supernate at the Hanford Waste Treatment and Immobilization Plant (WTP). To support this goal, Washington River Protection Solutions (WRPS) is designing a system for suspended solids and cesium (Cs, all isotopes) removal from Hanford tank waste supernate. The Cs-decontaminated effluent will then be sent to the WTP Low-Activity Waste (LAW) facility for vitrification. The Cs removal is critical for eliminating the high dose rate associated with ^{137}Cs and facilitating a contact maintenance philosophy (i.e., manned entries and close proximity for material handling) at the LAW Facility. The maximum ^{137}Cs concentration in the LAW sent to the WTP is targeted to be below $3.18\text{E-}5\text{ Ci }^{137}\text{Cs/mole of Na}$; this is termed the waste acceptance criteria (WAC) limit.¹ The filtration and ion exchange systems will be placed near the Hanford tanks and are collectively termed the Tank-Side Cesium Removal (TSCR) system. The ion exchange media selected for Cs removal at TSCR is crystalline silicotitanate (CST) that is manufactured in a nearly spherical form by Honeywell UOP LLC (UOP; Des Plaines, IL) as product IONSIV™ R9140-B.

Small-scale efficacy testing of CST is needed with Hanford tank waste to assess and resolve issues before committing the waste to full scale plant processing. Small scale testing is conducted with small exchange bed volumes (BVs; e.g., 10 mL) in small diameter columns. This scale accommodates safe transport of limited volumes of high-activity tank waste and associated handling in hot cells. However, Cs exchange load behavior at the small-scale processing format may not exactly mirror exchange behavior at the pilot or plant scales. For example, spherical resorcinol formaldehyde testing comparison with 10-mL and full-scale columns showed strikingly different transition zones associated with rate limiting parameter of film diffusion (Fiskum et al. 2019a) while holding all other affecting parameters (matrix, temperature, residence time) constant. Understanding this small-scale test effect was useful in assessing overall performance at full scale. A similar effort was needed for CST. Testing to date has used a variety of CST lot numbers, matrices, and process parameters confounding scaling comparisons, with one exception. Walker Jr. et al. (1998) tested Melton Valley W-27 supernate with 30 x 60 mesh CST (Lot 07398-38B) at the small-scale (1.5 cm internal diameter [ID] x 6 cm tall, 10-mL CST bed) and full-scale (30 cm ID x ~54 cm tall, 38 L CST bed). Unfortunately, the tank waste chemical composition was different between the small-scale and full-scale tests with respect to relevant impurities (such as Ba, Ca, K, and Pb), which could impact the Cs load profile. Comparison of the full-scale test load curves at flowrates of 3 BVs per hour (BV/h) and 6 BV/h showed early initial Cs breakthrough relative to the small-scale test load curve, with convergence ranging from 20% to 50% Cs breakthrough. For the W-27 waste material, the full-scale test had a longer mass transfer zone relative to the small-scale test. The performance difference at the two process scales cannot be separated from the differences in the feeds.

Several factors affect Cs exchange onto CST. Recent testing has shown different production lots of CST resulted in significant differences in Cs load characteristics (specifically Lot 2002009604 resulted in improved performance over Lot 2081000057). The feed volume processed (5.6 M Na simulant at 1.83 BV/h) to reach the WAC limit for these two CST lots differed by 61% (Fiskum et al. 2019b). The total Cs capacity tested with AP-107 tank waste between the two lots differed by 13% (Fiskum et al. 2019c). Testing has also shown that residence time significantly influences the efficacy of Cs uptake (Fiskum et al. 2019b) where increasing residence time in the CST bed improves Cs removal. This is evidence that the exchange kinetics at the exchange site is the rate limiting step in Cs ion exchange onto CST. Additionally, matrix effects also influence CST Cs capacity. Brown et al. (1996) showed that increasing Na concentration decreases Cs exchange capacity. Bray et al. (1995) showed that increasing pH from 10 to

¹ From *ICD 30 – Interface Control Document for Direct LAW Feed*, 24590-WTP-ICD-MG-01-030, Rev. 1, 2017, Bechtel National, Inc. (River Protection Project Waste Treatment Plant), Richland, Washington.

>14 caused a concomitant decrease in the Cs exchange capacity. Trace metals, such as Ba, Ca, Fe, Pb, Pu, Sr, U, and Zn, in caustic solution have also been shown to exchange or adsorb onto the CST (Walker Jr. et al. 1998, King et al. 2007, and Campbell et al. 2019).

UOP has produced CST for use in full scale columns at various mesh sizes (e.g., 18 x 50, 25 x 40, 30 x 60). Particle diameter is important to small scale columns where wall effects or channeling may occur with large particles. Optimally, >30 particle diameters should bridge across the bed diameter to mitigate wall effects (Harland, 1994). For a 15 mm diameter column, the ideal average particle size distribution (PSD) should not exceed 500 μm . The CST Lot 2002009604 was provided as the 18 x 50 mesh size. Note that 18 mesh screen allows particles up to 1 mm diameter to pass. This screening out of large particles is important to successful narrow column testing.

Fiskum et al (2019b) demonstrated scalability of the Cs load curve for a full-height CST bed (226 cm tall x 2.54 cm ID) to a 12% height CST bed (27 cm tall x 1.44 cm ID). The full-height column used 18 x 50 mesh CST as provided by UOP. The 12% height bed used <25 mesh sieve fraction of the CST, removing all particles >710 μm (41 wt% removed). This effort was intended to provide a closer match of particle numbers across the bed diameters. Based on the d_{50} measured particles sizes, the full-height column had ~36 particles across the diameter and the 12% height column had ~24 particles across the column diameter. Cs load curves were generated using a single production lot of 5.6 M Na simulant tank waste solution at 1.83 BV/h. The Cs load curves matched nearly perfectly with respect to the WAC limit (240 BVs) and the extrapolated 50% Cs breakthrough (~1000 BVs). The step-down in the CST sieve fraction was considered key in matching the Cs breakthrough profiles. A similar sieve fraction downsize was investigated for the small-scale (10 mL BV, 2.5% height) column.

WRPS funded Pacific Northwest National Laboratory (PNNL) to conduct additional testing with small scale columns and 5.6 M Na simulant for direct comparison to the performance from the full height and 12% height columns. Two CST sieve fractions were tested in the small-scale single-column systems: <25 mesh that matched previously reported CST bed configuration and <35 mesh to assess the smaller sieve cut effects.

2.0 Quality Assurance

All research and development (R&D) work at PNNL is performed in accordance with PNNL's Laboratory-Level Quality Management Program, which is based on a graded application of NQA-1-2000, *Quality Assurance Requirements for Nuclear Facility Applications* (ASME 2000), to R&D activities. To ensure that all client quality assurance (QA) expectations were addressed, the QA controls of the PNNL's WRPS Waste Form Testing Program (WWFTP) QA program were also implemented for this work. The WWFTP QA program implements the requirements of NQA-1-2008, *Quality Assurance Requirements for Nuclear Facility Applications* (ASME 2008), and NQA-1a-2009, *Addenda to ASME NQA-1-2008* (ASME 2009), and consists of the WWFTP Quality Assurance Plan (QA-WWFTP-001) and associated QA-NSLW-numbered procedures that provide detailed instructions for implementing NQA-1 requirements for R&D work.

The work described in this report was assigned the technology level "Applied Research" and was planned, performed, documented, and reported in accordance with procedure QA-NSLW-1102, Scientific Investigation for Applied Research. All staff members contributing to the work received proper technical and QA training prior to performing quality-affecting work.

3.0 Test Conditions

This section describes the CST media, 5.6 M Na simulated waste, and column ion exchange conditions. All testing was conducted in accordance with a test plan prepared by PNNL and approved by WRPS¹ and a test instruction.²

3.1 CST Media

WRPS purchased ten 5-gallon buckets (149 kg total) of IONSIV™ R9140-B³, Lot number 2002009604, material number 8056202-999, from Honeywell UOP LLC (Des Plaines, IL). This CST production lot was screened by the manufacturer to achieve an 18 x 50 mesh size product. The product was requested to be delivered to WRPS in a series of 5-gallon buckets (as opposed to a 50-gallon drum) to aid in material distribution, handling, and sampling at PNNL. The CST was transferred from WRPS to PNNL on September 20, 2018, under chain of custody. Once received, the CST was maintained at PNNL in environmentally controlled spaces. One of the 5-gallon buckets containing CST was delivered to the PNNL Radiochemical Processing Laboratory. The handling and splitting of the CST were previously described (Fiskum et al. 2019b). A suitably sized sample split was subsampled for the current testing.

A 50.7-g subsample was collected and passed through a 25-mesh sieve (ASTM E11 specification) as previously described (Fiskum et al. 2019b). A mass fraction of 46% (23.3 g) passed through the sieve and was collected. This mass fractionation was consistent with previous tests (Fiskum et al. 2019b, 2019c).

A 327-g subsample was collected for sieving through a 35-mesh sieve (ASTM E11 specification). The CST sample was first divided into fourths for stepwise sieving; the entire mass was too unwieldy for a single 12-inch diameter sieve. Each sieve was shaken by hand until the mass collection on the catch pan was essentially constant. An average mass fraction of 17% (56.8 g) passed through the 35-mesh sieves.

Both CST sieve fractions were pretreated by contacting with 100 mL of 0.1 M NaOH three and five successive times for the <25 mesh and <35 mesh sieve fractions, respectively. The 0.1 M NaOH rinse solution and colloidal fines from the CST were decanted. The bulk of the rinsed CST was maintained with an overburden of 0.1 M NaOH.

A nominal 10-mL fraction of each CST slurry was removed for particle size analysis (PSA). The PSA was conducted using a Malvern Mastersizer 2000 coupled with a HydroG dispersion unit. Measurements were collected pre-sonication, during sonication, and post-sonication. It was observed that applied sonication had marginal impact on the PSD (see Appendix B).

Duplicate 10-mL fractions of the <35 mesh sieve fraction were further collected for physical property testing inclusive of bulk density, bed density, and bed void fraction. The CST samples were rinsed once with deionized (DI) water to remove the bulk of the salt solution and were then dried for approximately two days in air at room temperature to evaporate interstitial water. The CST was then dried to constant mass at 100 °C. The dried CST was added incrementally to a known volume and mass of DI water in a

¹ Fiskum SK. 2019. TP-DFTP-064, Rev. 0.0 *DFTP Technology Testing and Support: Small Scale Column Tests with Crystalline Silicotitanate and 5.6 M Sodium Simulant*. Pacific Northwest National Laboratory, Richland Washington. Not publicly available.

² Fiskum, SK. 2019. *Cesium Removal from 5.6 M Na Simulant Using Crystalline Silicotitanate Using 10-mL Columns*. TI-DFTP-065. Pacific Northwest National Laboratory, Richland, Washington. Not publicly available. Implemented July 2019.

³ R9140-B is provided in the sodium form by the vendor.

25-mL graduated cylinder. As noted previously (Fiskum et al. 2019b), effervescence was observed upon initial contact with water. The CST was gently mixed by turning and slightly tipping the graduated cylinder, allowing free release of the gas. CST addition was paused to allow effervescence to complete before adding the next increment. After all effervescence ceased, the CST was tapped to final constant volume (V_{sl}). The headspace water was removed, the gross mass was measured, and the net slurry mass (M_{sl}) was calculated. The dry mass of CST (M_{CST}) was subtracted from the net slurry mass; the difference was ascribed to the water content in the slurry volume. This water included water in the CST crystalline interstices. The void fraction (VF) was calculated according to Eq. (3.1).

$$VF = \frac{M_{sl} - M_{CST}}{V_{sl}} \quad (3.1)$$

Table 3.1 provides the physical properties measured on CST Lot 2002009604 for the various sieve cuts tested (Fiskum et al. 2019b and current tests). The mass used for the density calculations was based on dried CST at 100 °C. With the exception of the PSDs, the physical properties were essentially the same, within experimental uncertainty of a couple of percent. The pre-sonication particle diameters were slightly larger than those of the post-sonication measurement (see Appendix B).

Table 3.1. Physical Properties of Washed R9140-B CST Lot 2002009604

Parameter	Fiskum et al. (2019b)		Current Report	
	Full Height	12% Height	2.5% Height	2.5% Height
Sieve cut for testing	Unsieved	<25 mesh	<25 mesh	<35 mesh Sample/duplicate
Bulk density, g/mL	1.01	1.02	nm	1.05/1.03
CST bed density, g/mL	1.00	1.01	nm	1.01/1.01
Settled bed void volume, %	67.6	66.2	nm	65.1/65.5
Cumulative particle undersize fractions, microns ^(a,b)	d_{10} : 394 d_{50} : 633 d_{90} : 955	d_{10} : 405 d_{50} : 567 d_{90} : 795	d_{10} : 433 d_{50} : 593 d_{90} : 816	d_{10} : 351 d_{50} : 479 d_{90} : 651
Column ID, cm	2.54	1.44	1.50	1.50
Cross section d_{50} particle #	40.1	25.4	25.3	31.3

(a) Volume basis, post-sonication.
(b) The sample and duplicate average values for full and 12% height samples from Fiskum et al. (2019b) are shown.
nm = not measured

Table 3.1 also shows the test column ID and the corresponding theoretical cross section of the post-sonicated d_{50} size particles. Optimally, at least 30 beads across the column diameter minimizes wall effects and channeling (Helfferich 1962). Testing at the full height 18 x 50 mesh CST and the 2.5% height <35 mesh CST met this threshold. Testing with <25 mesh CST pushed below the lower limit of this goal.

3.2 5.6 M Na Simulant

PNNL contracted the production of 680 gallons of 5.6 M Na simulant to Noah Technologies, Inc. (San Antonio, Texas). The simulant preparation was conducted as defined by Russell et al. (2017), with the exception that the Cs concentration was set to 8 µg/mL (instead of 13.8 µg/mL). This Cs concentration approximated the Cs concentration in AP-107 Hanford tank waste and matched simulant testing reported by Fiskum et al. (2018). The sodium oxalate component was omitted to mitigate solids precipitation. The target component masses and calculated ionic species concentrations are provided in Table 3.2. The reagents used to make the simulant were assayed at 99.2% or better. However, the sheer scale of the

production process required very large quantities of salts to be used, and a small metal impurity fraction could result in kilogram quantities of insoluble metal hydroxides. Thus, Noah Technologies was directed to wait at least 24 h after mixing and then filter the simulant through a 0.45-micron pore size filter. The simulant was prepared in one large lot to support full height and 12% height testing previously described (Fiskum et al. 2019b). A slight overage was requested to support rework (in case it was required) or follow-on work (as described herein).

Table 3.2. 5.6 M Sodium Simulant Target Composition (Fiskum et al. 2019b)

Component	Component Formula Weight (g/mole)	Target Component Mass per kg Solution (g)	Composition, g Component/ L Solution	Anion / Cation Species	Target Conc. (M)
Al(NO ₃) ₃ •9H ₂ O	375.13	49.82	62.27	Al as Al(OH) ₄ ⁻	0.166
NaOH (50%, w/w)	40.00	132.73	165.91	free OH ⁻	1.41
CsNO ₃	194.91	0.0094	0.0117	Cs ⁺	6.00E-05
KCl	74.55	7.28	9.10	K ⁺ and Cl ⁻	0.122
Na ₂ SO ₄	142.04	7.51	9.39	SO ₄ ²⁻	0.0661
NaNO ₂	69.00	56.30	70.38	NO ₂ ⁻	1.02
NaNO ₃	84.99	87.17	108.97	NO ₃ ⁻	1.78
Na ₃ PO ₄ •12H ₂ O	380.12	13.14	16.42	PO ₄ ³⁻	0.0432
Na ₂ CO ₃	105.99	46.33	57.91	CO ₃ ²⁻	0.467
DI water	18.02	598.35	747.94	Na ⁺	5.60

A 22-L aliquot of the simulant was collected and spiked with 0.19 mCi ¹³⁷Cs tracer to reach a final ¹³⁷Cs concentration of 8.69E-3 μCi/mL. A 10-mL sample collection allowed for a calculated decontamination factor of ~60,000 when measured by gamma energy analysis (GEA). The ¹³⁷Cs tracer was mixed into solution using a recirculating pump for a total of 100 minutes. An inline Whatman 5-micron pore size monofilament anisotropic polypropylene capsule filter (Polycap 36 HD) was installed to remove any solids suspended during mixing. A simulant sample was collected after 80 min of mixing time and again after an additional 20 min of mixing to assess that the activity concentration was constant. After mixing, the simulant stood for an additional six days; this ensured the tracer equilibrated with the simulant Cs. The total Cs mass in the tracer was insignificant relative to the native Cs in the simulant.

3.3 Ion Exchange Process Testing

This section describes the ion exchange column system and 5.6 M Na simulant processing conditions.

3.3.1 Ion Exchange Column System

Each test used an independent ion exchange system consisting of a single column. Figure 3.1 and Figure 3.2 provide schematics of the two ion exchange process systems. The <35-mesh CST was tested without inline detection (Figure 3.1). The <25-mesh CST was tested with the addition of in-line gamma detectors (two LaBr₃ and one NaI) (see Figure 3.2). Except for the long loop through the inline detection system, the two ion exchange assemblies were configured as closely as possible to each other.

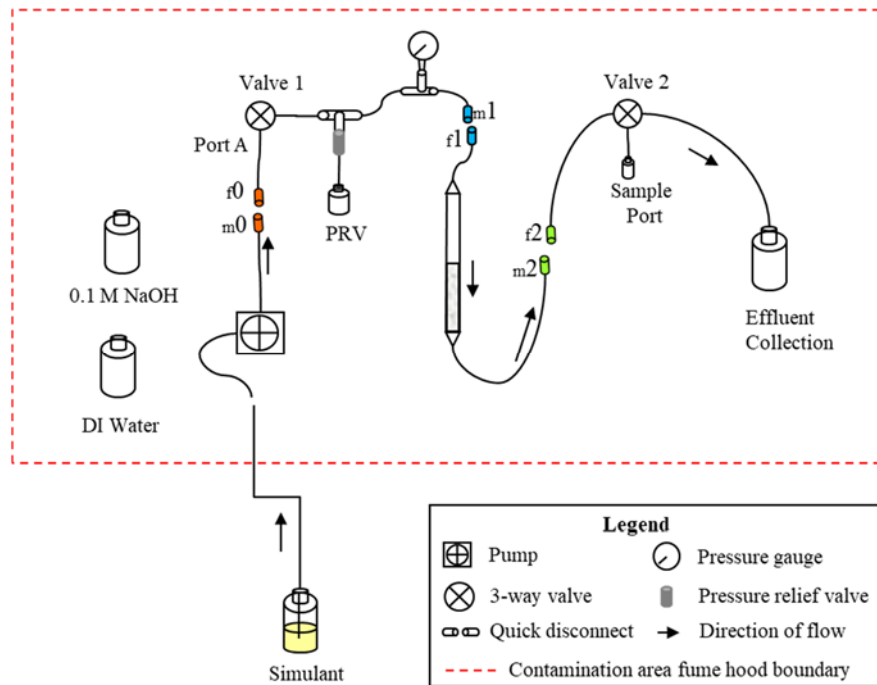


Figure 3.1. Ion Exchange System Schematic <35 mesh CST (Color Code Green)

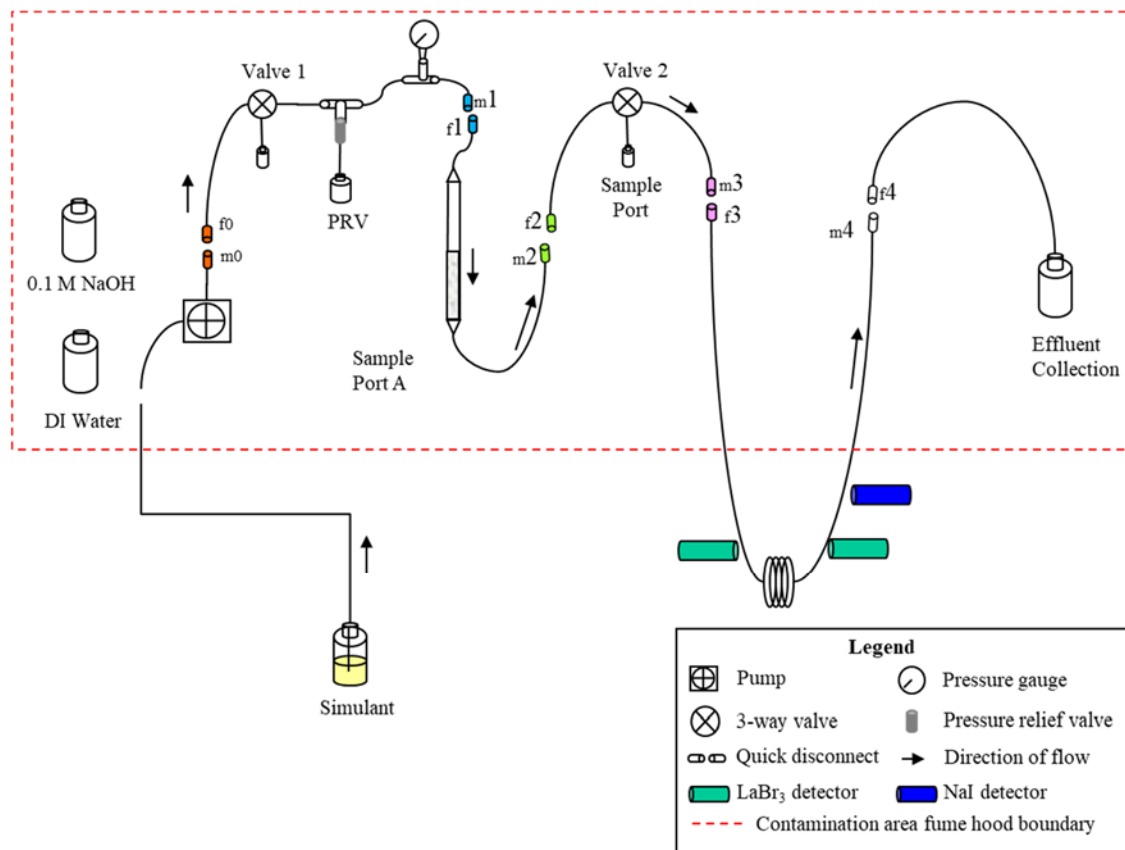


Figure 3.2. Ion Exchange System Schematic <25 mesh CST with Inline Gamma Detection (Color Code Purple)

Figure 3.3 and Figure 3.4 show photographs of each system after installation in the fume hood. Fluid flow through the system was controlled with a Fluid Metering Inc. positive displacement pump; flowrate was controlled remotely with the associated stroke rate controller. Fluid was pumped past a Swagelok pressure relief valve with a 10-psi trigger point and an Ashcroft pressure gage. The 1/8-inch outside diameter / 1/16-inch inside diameter polyethylene tubing was purchased from Polyconn (Plymouth, MN). The 1/8-inch outside diameter / 1/16-inch inside diameter stainless steel tubing was used in conjunction with the valve manifold and as dip tube in the feed reservoir. Valved quick disconnects were purchased from Cole Parmer (Vernon Hills, IL). Use of the quick disconnects enabled easy flow re-routing, as needed. The quick disconnects were color-coded to ease correct installation.

Chromaflex[®] column assemblies were custom-ordered from Kimble Chase (www.kimble-chase.com). Each column assembly included the column plus the standard top and bottom end fittings. Each column was made of borosilicate glass; the straight portion of the column was 9 cm tall with an inside diameter of 1.5 cm (corresponding to a CST volume of 1.77 mL/cm). The columns flared at each end to support the off-the-shelf column fittings and tubing connectors that were composed of polytetrafluoroethylene. The CST was supported by an in-house constructed support consisting of a 200-mesh stainless steel screen tack welded onto a stainless-steel ring. A rubber O-ring was placed on the outside of the stainless steel support and the fitting was snug-fitted into place in the column; see Fiskum et al. (2018) for more detail. The flared cavity at the bottom of each column was filled to the extent possible with 4-mm-diameter glass beads to minimize the mixing volume below the CST bed (achieved 50% volume reduction from ~6 mL to ~3 mL). An adhesive centimeter scale with 1-mm divisions (Oregon Rule Co. Oregon City, OR) was affixed to the column with the 0-point coincident with the top of the support screen.

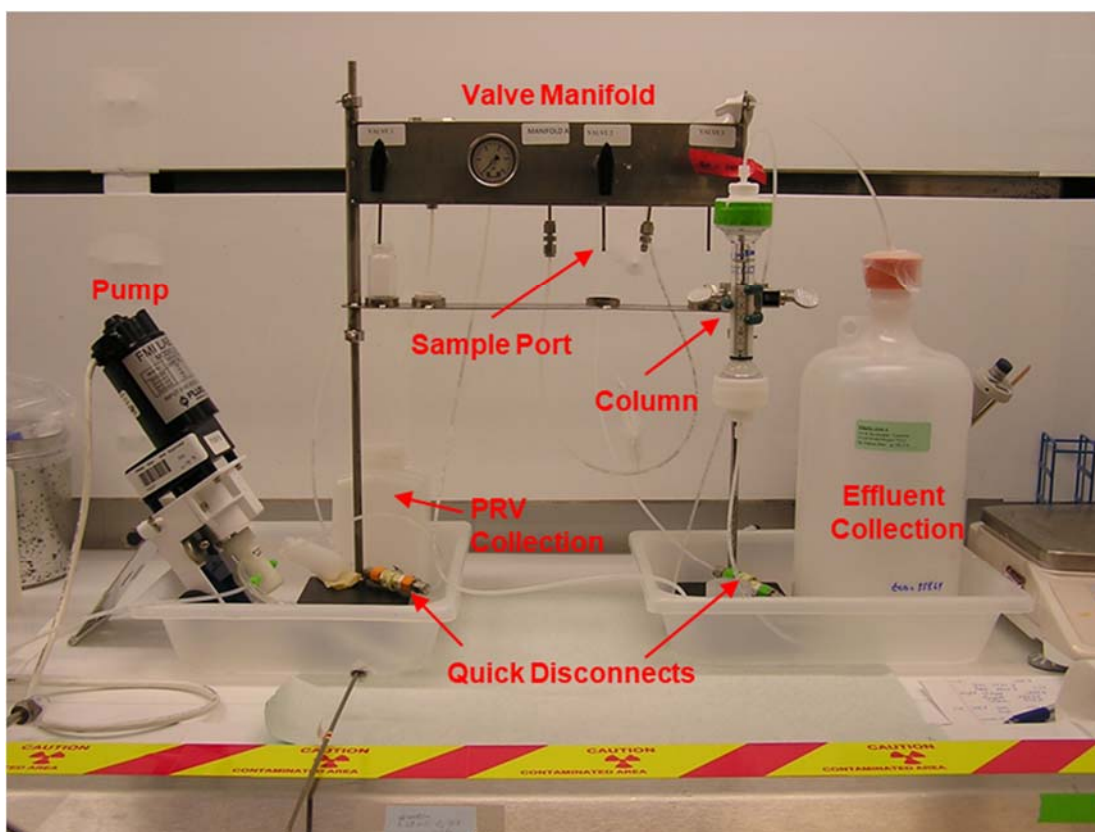


Figure 3.3. Photograph of Ion Exchange System, <35-mesh CST, Color Code Green

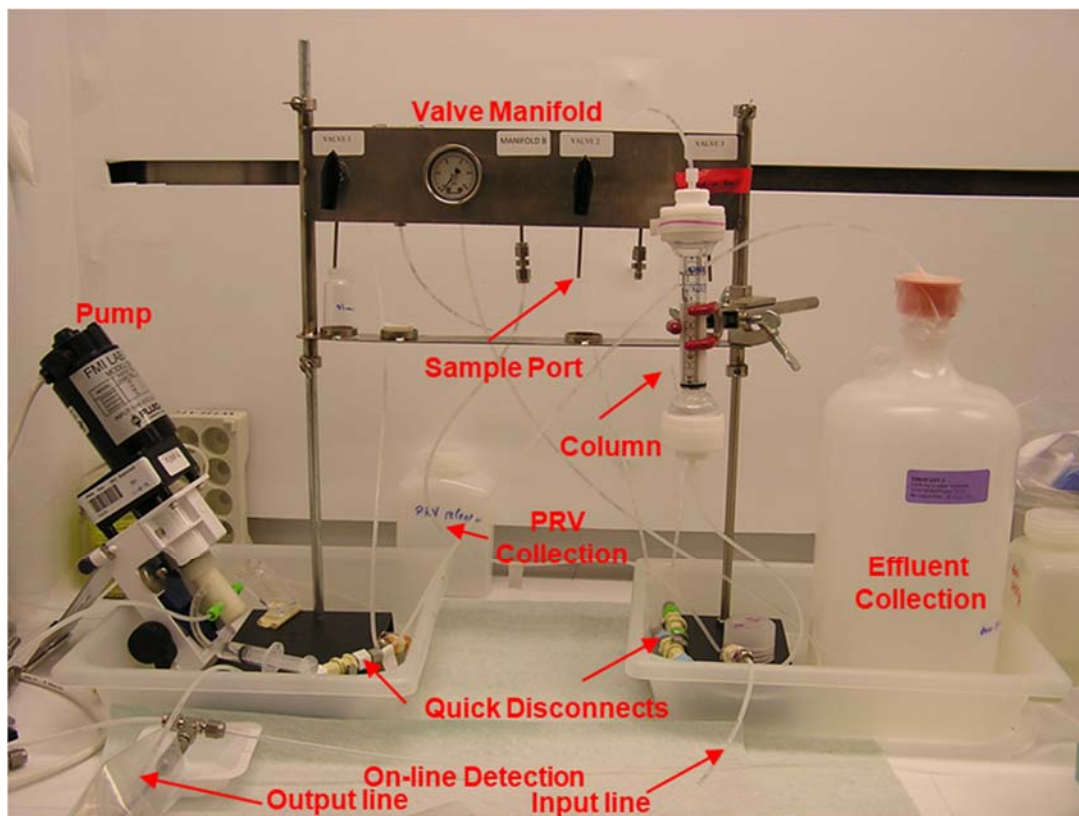


Figure 3.4. Photograph of Ion Exchange System, <25-mesh CST, Color Code Purple

Three Swagelok valves were installed in the valve manifold; only the first two valves were used to support the single column test. (The third valve supports sampling from a lag column.) Valve 1 was used to isolate the column from the system (when in the closed position) and purge the tubing from the inlet to valve 1 (when placed in the sampling position). Samples from column loading, the feed displacement (FD), and the water rinse were collected at valve 2. The gross simulant effluent was collected at the effluent line into a 1-gallon polyethylene bottle. During sample collection, the effluent bottle was capped and then weighed to assess the total mass (and hence volume and flowrate) collected between sampling periods.

The system was filled with water and then slightly pressurized to confirm system leak tightness. The pressure relief valve was confirmed to trigger at the manufacturer set point (10 psig). Water was removed from the columns and replaced with 0.1 M NaOH. A 10.0-mL aliquot of settled CST was measured using a 10-mL graduated cylinder and quantitatively transferred to the column. The CST was allowed to settle through the 0.1 M NaOH solution in the column, thus mitigating gas bubble entrainment. The column was tapped with a rubber bung until the CST height no longer changed.

The CST BV corresponded to the settled CST volume as measured in the graduated cylinder prior to transferring it into the ion exchange column. The reference CST BV was 10.0 mL. The settled CST bed heights in the columns were ~5.85 cm as measured from the adhesive cm scale. This CST height corresponded to 2.5% of the full height column (234 cm). The fluid above the bed was set at the 8 cm mark corresponding to a 3.8 mL volume above the surface of the bed.

The entire fluid-filled volume of the <35 mesh CST assembly (Green) was ~26 mL, inclusive of fluid in the CST beds. The entire fluid filled volume of the <25 mesh CST assembly (Purple) was ~42 mL. The

fluid fraction in the CST bed was 65% to 66% (Table 3.1). Therefore, the predominant source of mixing fluid was in the CST bed itself, at ~6.8 mL fluid, followed by the fluid head above the CST bed at ~3.8 mL and then the fluid just below the CST bed at ~3 mL. The Purple system also incorporated ~790 cm of $\frac{1}{16}$ -inch ID tubing supporting in line gamma detection. This corresponded to ~16 mL of additional fluid volume; however, this narrow column geometry was not considered a mixing chamber. Thus, ~52% (Green) and 33% (Purple) of the total fluid holdup volume was unavoidably associated with the column geometry itself and was, to some extent, a mixing chamber. These fluid mixing volume fractions are not likely to be representative of plant-scale operations.

3.3.2 Processing Conditions

Once the CST-loaded columns were installed in the manifold system, a flow of 0.1 M NaOH was used to verify the system integrity (leak tightness) and calibrate the pump. Feed was pumped from the feed carboy located below the fume hood and processed through the columns. During the loading phase, nominal 10-mL samples were collected from each column at the sample collection port. Samples were collected after the first ~11 BVs were processed and again at nominal 44-BV (~24-h) increments. Flowrate checks and pump stroke rate controller adjustments were made more frequently at the beginning of the process run and as needed throughout run.

After simulant loading was completed, ~6 BVs of 0.1 M NaOH FD were passed downflow through the system to rinse residual feed out of the column and process lines through valve 2. The FD was collected in 10-mL increments from valve 2. The 6 BVs was equivalent to ~2 times the fluid-filled apparatus volume (AV) through valve 2 (not including the gamma detection loop). The system was then rinsed with ~12 BVs of DI water. The water rinse was collected in 20-mL increments from valve 2.

Because all rinse solutions were collected from valve 2, the lines following valve 2 were still filled with simulant containing ~50% of the feed ^{137}Cs concentration. These lines needed to be flushed or replaced to obtain a representative ^{137}Cs measurement in the final system flush solution. The Green system effluent line between valve 2 and the effluent collection container was replaced to remove residual feed from the system and 10 mL water was then processed through the effluent line to clear out residual feed in valve 2. The Purple system column was bypassed (by realigning the quick disconnects *m1* to *f2*) to allow a water flush through the gamma detection lines. An 86-mL volume of water was washed through the lines, collecting the flush water at the effluent line; the tubing connections were re-established, bringing the column back in line. Each system was connected to an argon gas source at the *f0* quick disconnect (see Figure 3.1 and Figure 3.2). A slight pressure of argon was applied to purge the systems of drainable fluid; purging continued until no more fluid was collected. The collected volume did include the interstitial fluid space between the CST beads, but did not include fluid in the CST pore space.

All processing was conducted at ambient temperature conditions, nominally $21\text{ }^{\circ}\text{C} \pm 2\text{ }^{\circ}\text{C}$. Test parameters, including process volumes, flowrates, and CST contact times, are summarized in Table 3.3 and Table 3.4. The pump head stroke length was adjusted to maintain the flowrate at 1.83 BV/h. Flowrate through the Green system was well controlled. Maintaining the flowrate through the Purple system was more challenging. Salt buildup in the pump head appeared to cause a decrease in pumping efficiency after processing ~315 BVs, as evidenced by decreasing flowrates despite increasing stroke rates. After processing ~658 BVs, the exterior pump head surface was rinsed, breaking up some observed salt buildup. This apparently improved pump head performance, as the flowrate ratcheted up significantly. The flowrate was monitored more closely and the stroke rate adjusted accordingly. Figure 3.5 and Figure 3.6 show the achieved flowrates as a function of time. The flowrates reported in Table 3.3 and Table 3.4 are time-weighted averages.

Table 3.3. Experimental Conditions for <35 Mesh CST (Green) Processing, August 5 to August 28, 2019

Process Step	Solution	Volume			Flowrate		Duration (h)
		(BV)	(AV) ^(a)	(mL)	(BV/h) ^(b)	(mL/min) ^(b)	
Loading	Simulant	1003	NA	10,030	1.83	0.304	555
Feed displacement	0.1 M NaOH	5.52	2.33	55.2	2.94	0.489	1.9
Water rinse	DI water	11.9	5.04	119	2.96	0.494	4.0

(a) AV up to valve 2: ~24 mL to valve 2.

(b) Time-weighted average flowrates.

BV = bed volume (10.0 mL as measured in graduated cylinder).

AV = apparatus volume

NA = not applicable

Table 3.4. Experimental Conditions for <25 Mesh CST (Purple) Processing, August 5 to August 28, 2019

Process Step	Solution	Volume			Flowrate		Duration (h)
		(BV)	(AV) ^(a)	(mL)	(BV/h) ^(b)	(mL/min) ^(b)	
Loading	Simulant	1014	NA	10,137	1.83	0.305	555
Feed displacement	0.1 M NaOH	5.98	2.65	59.8	3.15	0.524	1.9
Water rinse	DI water	12.2	5.39	122	3.02	0.503	4.0

(a) AV up to valve 2: ~23 mL up to valve 2.

(b) Time-weighted average flowrates.

BV = bed volume (10.0 mL as measured in graduated cylinder).

AV = apparatus volume

NA = not applicable

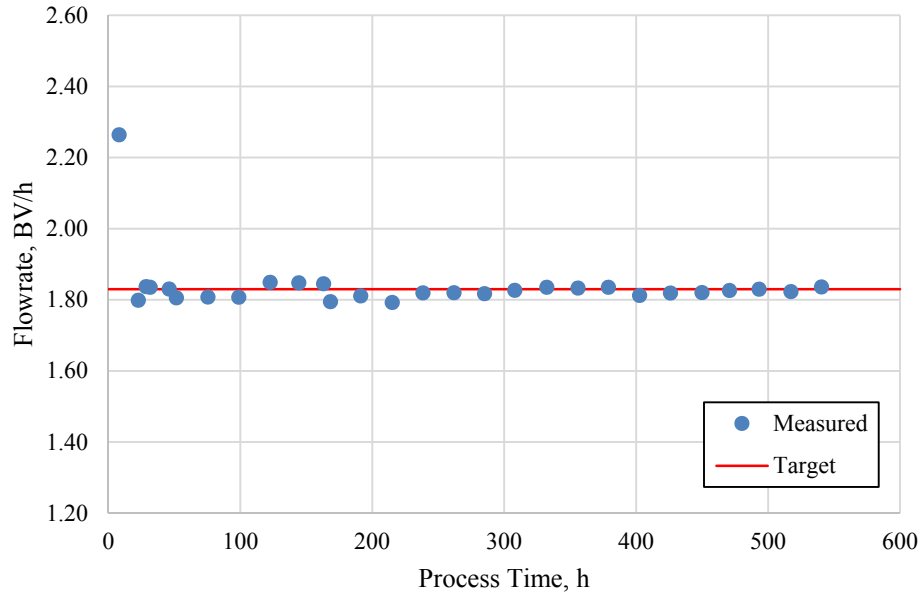


Figure 3.5. <35 Mesh (Green) Flowrate as a Function of Process Time

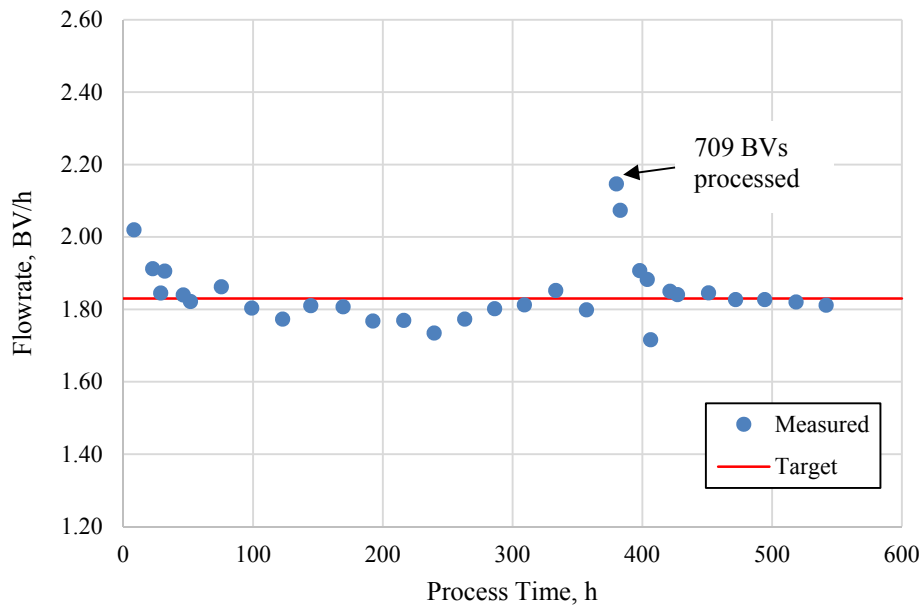


Figure 3.6. <25 Mesh (Purple) Flowrate as a Function of Process Time

These two simulant process cycles mimicked, as best as possible, the process flow anticipated during small scale testing in the hot cell with actual tank waste as well as the TSCR facility in terms of BV/h (i.e., contact time), FD, and water rinse. It was understood that the feed superficial flow velocity in this small-column configuration (0.17 cm/min) could not begin to match that of the full-height processing configuration (7.3 cm/min, Fiskum et al. 2019b).

3.4 Analysis

Two 10-mL samples of the feed solution were collected and analyzed by GEA to determine the baseline feed ^{137}Cs concentration. The collected 10-mL samples (loading and FD) were analyzed directly to determine the ^{137}Cs concentration using GEA. The water rinse samples (20-mL each) and effluents were subsampled for GEA. Cesium loading breakthrough curves were generated based on the feed ^{137}Cs concentration (C_0) and the effluent Cs concentration (C) in terms of % C/C_0 .

Samples were submitted to the Analytical Support Operations (ASO) and were analyzed directly (no preparation) by GEA. Each sample was counted long enough to provide a nominal 1% count uncertainty. Samples below $4\text{E-}5 \mu\text{Ci/mL}$ ^{137}Cs were counted ~ 23 h and uncertainties were much higher. All analyses were conducted by the ASO according to a standard operating procedure, the ASO QA Plan, and the Analytical Service Request.

In addition to discrete sample collection, on-line detection was conducted on the <25 mesh CST column effluent (Purple system). A full description of the configuration, process constraints, and analysis results are provided in Appendix C.

4.0 Column Processing Results

This section discusses the Cs exchange behavior during the load, FD, water rinse, and final solution flush from the system. Raw data are provided in Appendix A.

4.1 Cs Loading, Feed Displacement, and Water Rinse

The 5.6 M Na simulant feed was processed at nominally 1.83 BV/h through one of two CST screened fractions, <25 mesh and <35 mesh. Figure 4.1a and Figure 4.2a show linear-linear plots of the cesium load profiles for feed processed through each column. The abscissa shows the BVs processed and the ordinate shows the effluent Cs concentration (C) relative to the feed concentration (C₀) in terms of % C/C₀. The C₀ values for ¹³⁷Cs was 8.69E-3 μCi/mL and the total Cs was 8.0 μg/mL. In this graphing layout, the Cs breakthrough appeared to start at ~270 BVs and 350 BVs for the <25 mesh and <35 mesh CST columns, respectively.

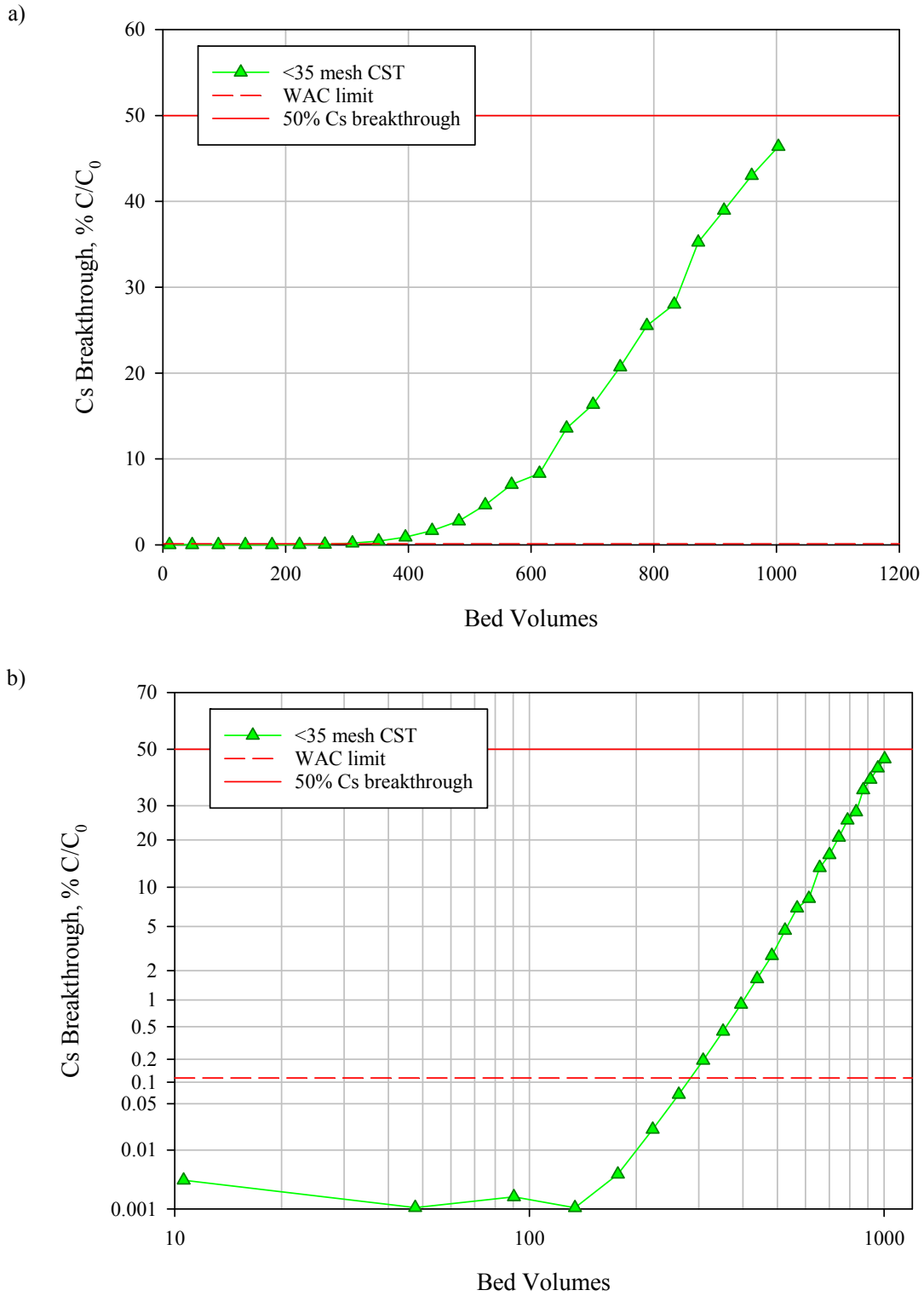
Figure 4.1b and Figure 4.2b show the same Cs load data provided in Figure 4.1a and Figure 4.2a, but with the ordinate % C/C₀ on a probability scale and the abscissa BVs processed on a log scale. Under normal load processing conditions, these scales provide a predictable straight-line Cs breakthrough curve and provide greater fidelity of load characteristics at low and high % C/C₀ values (Buckingham 1967). In this graphing layout, the Cs breakthrough appeared to start at ~100 BVs and 140 BVs for the <25 mesh and <35 mesh CST columns, respectively. In addition to the 50% C/C₀ indication line, the WAC limit at 0.114% C/C₀ is also apparent (dotted red line).¹ The WAC limit Cs breakthrough occurred at 185 BVs for the <25 mesh CST and at 285 BVs for the <35 mesh CST.

The 50% Cs breakthrough was nearly reached after processing 1014 BVs (49% C/C₀) through the <25 mesh CST and 1003 BVs through the <35 mesh CST (46% C/C₀). The column data were evaluated to estimate the BVs to 50% breakthrough. The breakthrough curves were estimated by the error function (erf) (Hougen and Marshall 1947; Klinkenberg 1994):

$$\frac{C}{C_0} = \frac{1}{2} (1 + \operatorname{erf}(\sqrt{k_1 t} - \sqrt{k_2 z})) \quad (4.1)$$

where k₁ and k₂ are parameters dependent on column conditions and ion exchange media performance, t is time (or BVs processed), and z is the length of the column. Using this model, a fit was generated to the experimental data. The 50% breakthrough was estimated by multiplication of k₁ and k₂. Figure 4.3 shows the experimental data points with the curve fitted data for both column systems. The <25 mesh CST test extrapolated to 997 BVs to 50% breakthrough which was 1.7% lower than the experimental 1014 BVs at 49% breakthrough. It was noted that Cs breakthrough was flattening in the last four load samples, which was not accounted for by the model. The <35 mesh CST extrapolated to 50% Cs breakthrough was 1018 BVs. Isotherms with this CST lot and this simulant were not developed; thus, comparison cannot be made to the batch contact-predicted 50% breakthrough.

¹ The WAC limit was derived from the allowed curies of ¹³⁷Cs per mole of Na in the effluent to support contact handling of the final vitrified waste form—3.18E-5 Ci ¹³⁷Cs/mole Na. At 5.6 M Na and 156 μCi ¹³⁷Cs/mL (from AP-107, Rovira et al. [2018]) in the feed, the WAC limit is 0.114% C/C₀.



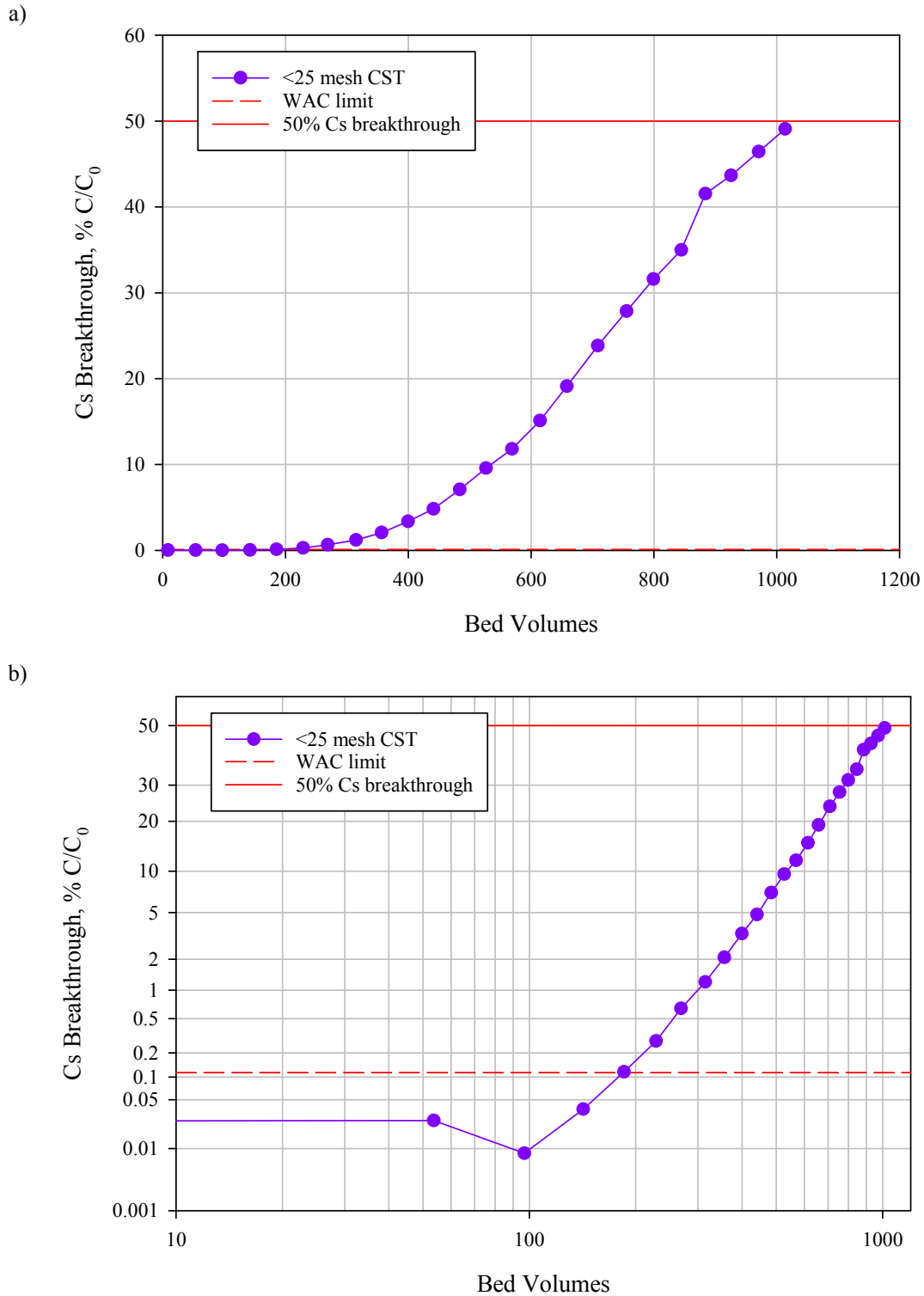


Figure 4.2. <25 Mesh CST with 5.6 M Na Simulant at 1.83 BV/h, a) Linear-Linear Plot, b) Probability-Log Plot

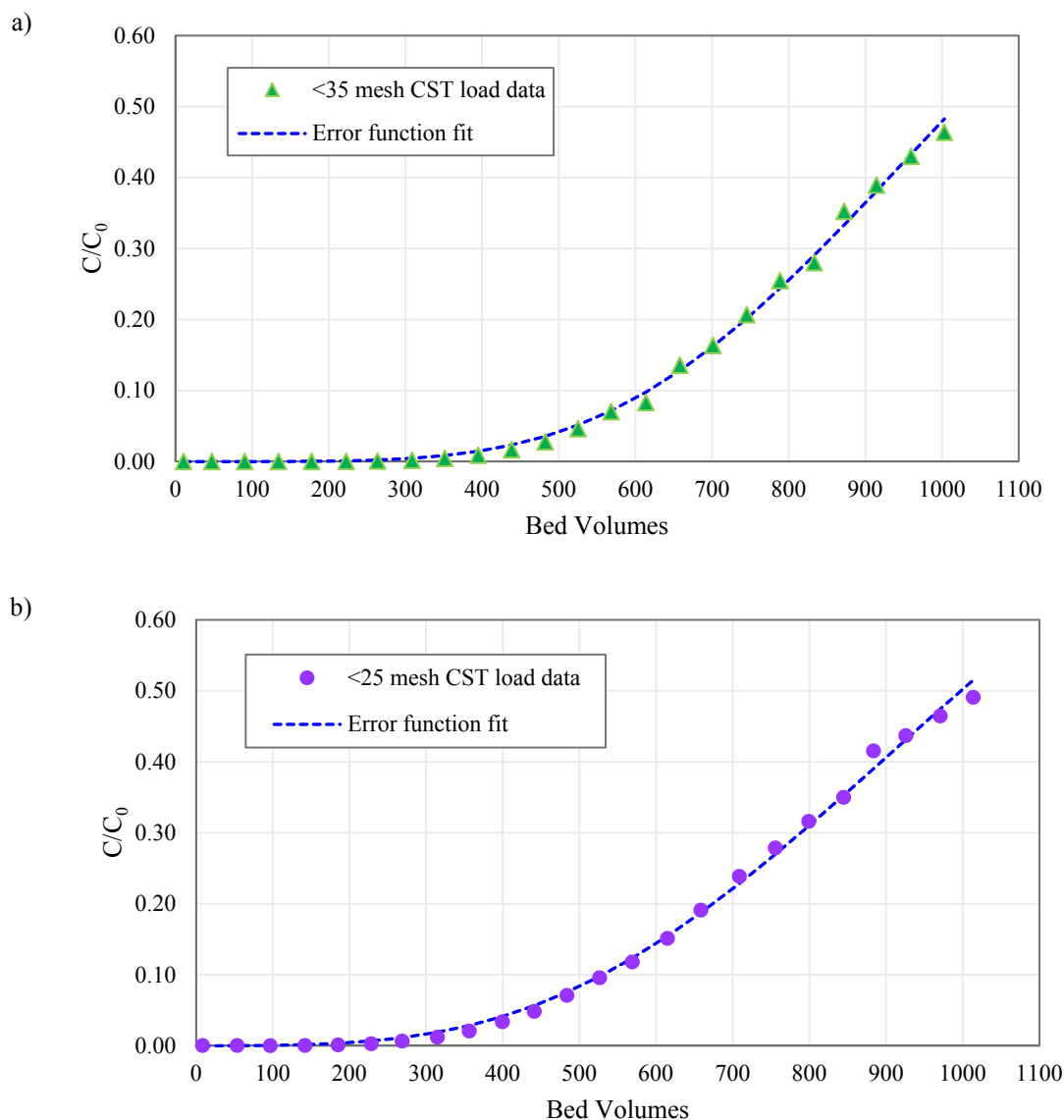


Figure 4.3. Extrapolated to 50% Breakthrough, a) <35 mesh CST, b) <25 mesh CST

The FD and water rinse ^{137}Cs (Cs) concentrations continued to decline with increasing process volume (see Appendix A). The final flushed fluid from the column system was slightly higher than that of the last water rinse sample; this increase may be associated with residual contamination in valve 2. This observation differed from previous work where ^{137}Cs concentration increased after processing most of the FD (Fiskum et al. 2019b and c). However, this system differed in that only a single column was tested and the column was loaded to nearly 50% Cs breakthrough; small leakage of Cs from the CST may have been masked by the Cs tailing from the column rinses.

4.2 On-line Detection Assessment

The on-line detection process only monitored the Cs load profile from the <25 mesh CST system through the load curve. The FD and water rinse samples were collected in totality from valve 2 before fluid was passed through the detectors. The on-line detection system results are provided in Appendix C.

4.3 Cs Load Performance Comparisons

The small-column Cs breakthrough data were compared (Figure 4.4) with the full-height lead column and 12% height column testing with 5.6 M Na simulant previously reported (Fiskum et al. 2019b). All significant parameters were held constant: CST production lot (Lot 2002009604), simulant production lot and associated chemical impurities, and the residence times in the CST bed (1.83 BV/h). The full-height column replicated the anticipated TSCR column height (234 cm). The 12% height column was 27 cm tall. At 5.8 cm tall, the CST beds used to process small scale tests were only 2.5% of the full-height TSCR column. Clearly the <25 mesh CST 2.5% height column resulted in early Cs breakthrough and the <35 mesh CST 2.5% height column resulted in late Cs breakthrough as benchmarked from the 12% and full height column tests. All load curves converged at 50% Cs breakthrough.

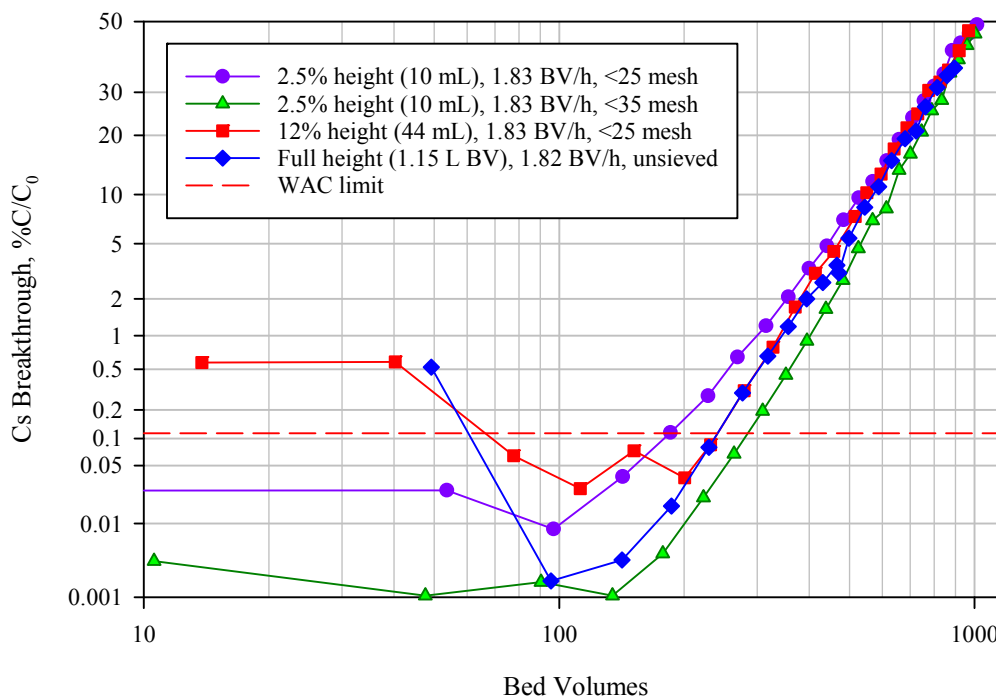


Figure 4.4. Cs Load Profile Comparisons, CST Lot 2002009604, 5.6 M Na Simulant

Figure note:

- The full height and 12% height performance data from Fiskum et al. (2019b).

As the size of the column is decreased from full height to 2.5% height, the CST particle size needs to be adjusted to balance the system performance. To maintain constant residence time, the superficial velocity is decreased, which results in a lower film mass transfer coefficient. For CST, the dominant resistance is the diffusion resistance inside the bead; however, film diffusion contributes to the overall mass transfer. As such, the adjustment of the particle diameter from 633 to 567 microns (<25 mesh) gave appropriate scaling when decreasing from full height (2.54 cm diameter column) to 12% height (1.44 cm diameter column). As expected, using the same particle size (<25 mesh) at 2.5% height (1.5 cm diameter column) resulted in slightly earlier Cs breakthrough. However, this testing showed that decreasing the mean particle diameter to 479 microns resulted in faster kinetics than observed at full height. These results suggest that the appropriate scaling for 2.5% height would be achieved with around 500 to 525 microns – or roughly <30 mesh.

Variation in dispersion was considered as a driving factor for the Cs breakthrough differences when shifting from the 12% height to the 2.5% height. However, this impact was thought to affect both 2.5% height tests (different sieve fractions) equivalently. Because their Cs breakthrough performances did not align, the film mass transfer was considered controlling.

The simulant Cs load behavior was compared to Hanford tank waste AP-107 (Fiskum et al 2019c) and AW-102 (Rovira et al. 2019) Cs load behaviors (lead columns) to assess performance given essentially identical column dynamics. Figure 4.5 provides both the linear-linear and probability-log plot of the load curves. Early Cs breakthrough behavior of the 5.6 M Na simulant in the 10-mL column appeared to shadow that of AW-102 and was also similar to that of AP-107. The similar nature of the early Cs breakthroughs indicate that full height processing of tank waste will be improved over that predicted by the small-scale test with respect to the WAC limit.

The simulant and AP-107 Cs load performances converged at ~240 BVs. After 240 BVs, the AP-107 load curve remained to the left of the 5.6 M Na simulant Cs load curve (lower Cs exchange). The AP-107 load performance offset from that of the simulant test was likely associated with 14% higher Cs concentration in AP-107 and additional impurity loading (e.g., Pb, Sr, Ba, U) consuming Cs exchange sites. The AW-102 load profile remained to the right of the simulant load profile. It is noted that the AW-102 test incorporated an 11-day stop-flow condition at 177 BVs¹ and the AW-102 Cs concentration was 30% lower than that of the simulant; both attributes extend the Cs breakthrough curve to the right.

¹ Rovira et al. (2019) reported that there appeared to be no detriment to column performance as a result of this unexpected pause.

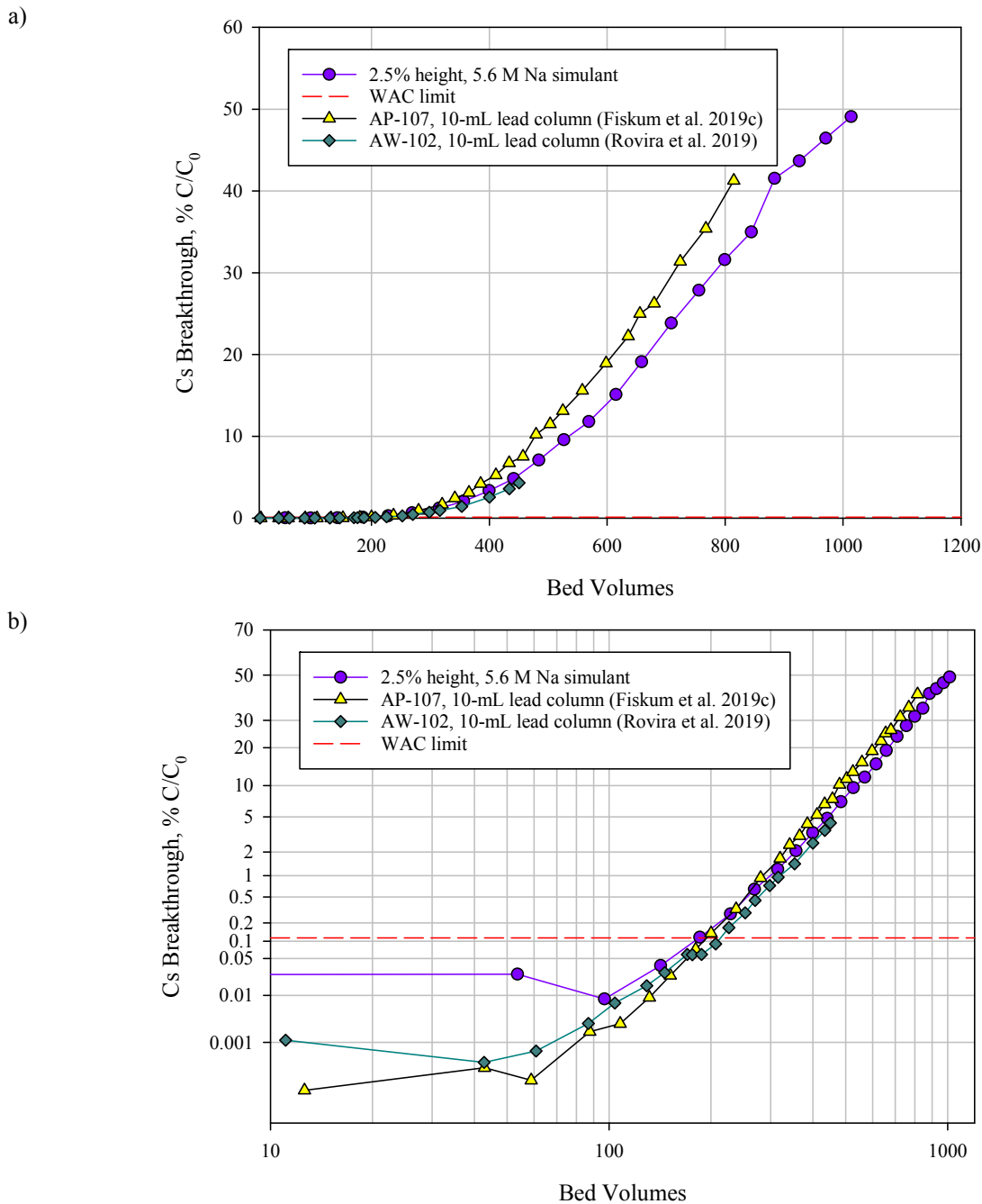


Figure 4.5. Comparison of Small-Scale Column Performance with <25 mesh CST and 5.6 M Na Simulant, AP-107, and AW-102, a) Linear-Linear Plot, b) Probability-Log Plot

Figure note--salient compositions of test matrices are as follows:

Analyte	AP-107 (Fiskum et al. 2019c)	AW-102 (Rovira et al. 2019)	Simulant
Cs	6.86E-5 M	4.63E-5 M	6.00 E-5 M
K	0.120 M	0.153 M	0.122 M
Na	5.97 M	5.83 M	5.60 M
Free hydroxide	0.89 M	0.98 M	1.41 M
Flowrate	1.88 BV/h	1.81 BV/h	1.83 BV/h

4.4 WAC Limit

Table 4.1 summarizes the WAC limit data for the current and previous data sets with the 5.6 M Na simulant and CST Lot 2002009604. The Cs load performance of the <25 mesh CST showed earlier breakthrough (55 BVs) than those observed at the 12% and full height column tests (Fiskum 2019b). The Cs load performance predictably improved for the <35 mesh CST (delayed by 55 BVs). The smaller CST particle size left a larger available surface area and shorter pore depth for Cs exchange and migration into the CST pores, improving Cs exchange kinetics on the CST.

Table 4.1. Comparison of BV to WAC Limit, 5.6 M Na Simulant

Test	WAC Limit (BVs)
2.5% height, <25 mesh CST	185
2.5% height, <35 mesh CST	285
12% height, <25 mesh CST	240
Full height, unsieved CST	240
Predicted from curve fit (Figure 4.6)	203
WAC limit 0.114% C/C ₀	

The amount of feed that can be processed before the effluent reaches the WAC limit is directly affected by the contact time the feed has with the CST bed. Thus, the effect of flowrate on BVs processed to the WAC limit is of special interest. Fiskum et al. (2019b) examined this effect using 5.6 M Na simulant solutions and found the BVs processed to the WAC limit versus the flowrate reasonably fit a power curve. In those evaluations, the test column systems were evaluated in segmented units or system volumes (SVs). Figure 4.6 plots the current data set with previously measured points in terms of total SVs processed per hour. The best fit curve was generated from the Fiskum et al. (2019b) data set. The measured <25 mesh CST WAC limit deviated by -10% from the projected WAC limit (from the curve fit). The <35 mesh CST WAC limit deviated from the projected curve by +29%.

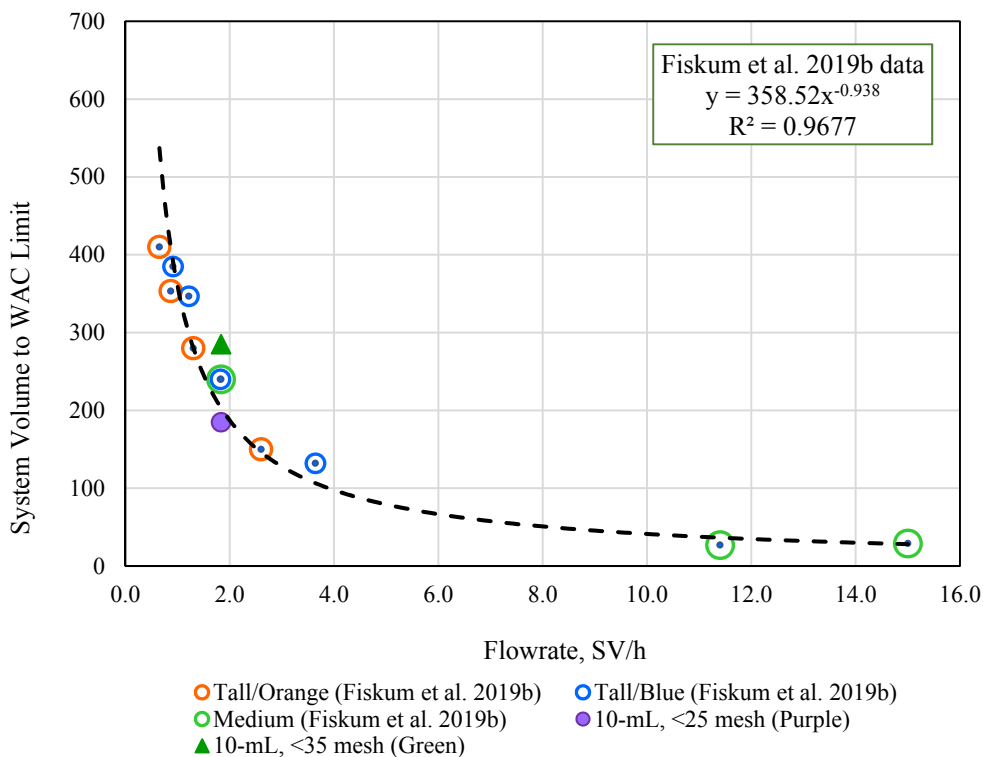


Figure 4.6. System Volume to WAC Limit vs. Flowrate

Figure notes:

- Fiskum et al. 2019b, 5.6 M Na simulant test matrix, CST Lot 2002009604.
 - Orange column data collected from four serial ~0.592-L CST beds.
 - Blue column data collected from four serial ~0.592-L CST beds.
 - Medium column data were collected from single 44-mL CST beds.

4.5 Cs Load Capacity

The quantities of ^{137}Cs loaded onto the columns were determined by subtracting the ^{137}Cs recovered in the samples and effluents from the ^{137}Cs fed to each column. About 85% of the total ^{137}Cs was loaded onto the <25 mesh CST bed and 88% of the total ^{137}Cs was loaded onto the <35 mesh CST bed. The total Cs loaded per g CST capacity was calculated according to Eq. (4.2).

$$\frac{A_{\text{Cs}} \times \text{CF}}{M} = C \quad (4.2)$$

where

- A_{Cs} = activity of ^{137}Cs , μCi on the column
- CF = conversion factor, mg Cs/ μCi ^{137}Cs
- M = mass of dry CST (10.0 g)
- C = capacity, mg Cs/g CST

Table 4.2 summarizes the total Cs loading onto each column and associated maximum Cs breakthrough. The total Cs loading for the 2.5% and 12% height tests were similar. The full height test showed lower

total Cs loading; however, comparison was confounded in that the total BV loading was 8% to 13% lower and the maximum Cs breakthrough was ~10% less. Both of these factors would result in less Cs exposure and exchange. Overall, the total Cs load capacity measured for the 2.5% height column was consistent with those of the larger columns.

Table 4.2. Comparison of Cs Loading onto CST, 5.6 M Na Simulant

Test	Process Volume (BVs)	Maximum Cs Breakthrough (% C/C ₀)	CST Cs Loading (mg Cs/g CST)	CST Cs Loading (mmoles Cs/g CST)
2.5% height, <25 mesh CST	1014	49.1	6.87	0.0517
2.5% height, <35 mesh CST	1003	46.4	7.04	0.0530
12% height, <25 mesh CST	967	47.3	6.95	0.0523
Full height, unsieved CST	895	36.5	6.60	0.0497

The difference in measured capacities between the <25 mesh and <35 mesh sizes was 2.5% and was likely within overall experimental uncertainty. Thus, at Cs saturation, the PSD in this mesh range was shown to not significantly impact total Cs capacity.

4.6 Mass Transfer Zone

The mass transfer zone is defined as the volume processed from the onset of Cs breakthrough to the full saturation of the ion exchanger where the effluent Cs concentration equals the influent Cs concentration. The 50% Cs breakthrough point is the inflection point around which the mass transfer zone pivots. The onset of Cs breakthrough can be interpreted in various ways. In this case two onset points, 5% and 20%, were evaluated for direct comparison to previously reported data.

In the current study, the columns were not quite loaded to 50% Cs breakthrough; the extrapolated 50% Cs breakthrough values were used (1018 BVs for <35 mesh CST and 997 BVs for <25 mesh CST). The number of BVs processed at 5% Cs breakthrough was determined from the load profile (generated in SigmaPlot[®] graphing program). The 20% Cs breakthrough values were calculated according to Eq. 4.1. The BV differences between 20% and 50% and 5% and 50% were calculated. These differences were doubled to determine the 20% to 80% and 5 to 95% Cs breakthrough mass transfer zones. Table 4.3 compares the mass transfer zones for processing with 5.6 M Na simulant on CST Lot 2002009604. Included in this comparison are the full height column (Blue) and 12% height column (Red) previously reported (Fiskum et al. 2019b). The 12% height and full height column 20% and 50% Cs breakthrough points were recalculated consistent with Eq. 4.1 to improve consistency in data manipulations.

Table 4.3. Mass Transfer Zone Comparison, CST Lot 2002009604, 1.83 BV/h, 5.6 M Na Simulant

Test	Flowrate (BV/h)	BVs to Cs Breakthrough			Mass Transfer Zone, BVs	
		(5%)	(20%)	(50%)	(20-80%)	(5 to 95%)
Full height/Blue, unsieved (Fiskum et al. 2019b)	1.82	492	708 ^(a)	1002 ^(a)	588 ^(a)	1020 ^(a)
12% height/ Red, <25 mesh (Fiskum et al. 2019b)	1.83	470	684 ^(a)	992 ^(a)	616 ^(a)	1044 ^(a)
2.5% height/Purple, <25 mesh	1.83	450	674	997	646	1094
2.5% height/Green, <35 mesh	1.83	532	744	1018	548	972

(a) The 20% and 50% Cs breakthrough values were re-evaluated based on Eq. (4.1).

The 2.5% height, <25 mesh CST column resulted in a slightly longer transition zone (~50 BVs) compared to the full and 12% height columns. The <35 mesh CST transition zone was ~100 BVs shorter than that of the <25 mesh CST. A transition zone match between the full height and 2.5% height columns appears to be in between the 25 and 35 mesh sieve cuts, i.e., 30 mesh sieve cut fraction.

5.0 Conclusions

Cesium ion exchange column testing with CST Lot 2002009604 was conducted to assess Cs exchange performance with 5.6 M Na simulated tank waste at the small (10-mL) column scale. This testing was conducted to assess the efficacy of relating small column testing, as required in hot cells on actual tank waste, to the full-height column processing.

Two single-column ion exchange systems were assembled, one containing <25 mesh CST and the other containing <35 mesh CST. A 5.6 M Na simulant, traced with ¹³⁷Cs, was passed through each system. The Cs load profile, Cs loading onto the CST, and Cs loading transition zone were determined. The following were observed.

1. The <25 mesh CST in the 10-mL column format resulted in earlier onset of Cs breakthrough compared to the 12% and full height columns. The earlier breakthrough was attributed to the slow superficial velocity negatively affecting film mass transfer.
2. The <35 mesh CST in the 10-mL column format resulted in later onset of Cs breakthrough compared to the 12% and full height columns. The smaller PSD and concomitant increased surface area improved the exchange kinetics.
3. The BVs processed to the WAC limit was artificially low when measured in the small column geometry compared to 12% and full height column geometries with <25 mesh CST. The <25 mesh CST resulted in reaching the WAC limit ~50 BVs sooner and the transition zone was ~50 BVs longer.
4. The <35 mesh CST reached the WAC limit ~45 BVs later and the transition zone was ~50 BVs shorter relative to the full height column test results. Switching to the smaller sieve cut improved the performance relative to the BV processed; however, use of the <35 mesh sieve cut overcorrected the Cs exchange performance relative to the 12% and full height tests.
5. Actual waste testing with AP-107 and AW-102 (reported by others) demonstrated early Cs breakthrough similar to that found with the simulant at the 2.5% height. This indicated that the full height performance in reaching the WAC limit with tank waste may be slightly better than predicted from the small-scale testing.

It is recommended that a 30-mesh sieve cut be tested to determine if it better reflects the 12% and full height column performances at the 10-mL BV scale. The goal is to use the most appropriate sieve cut CST in future actual tank waste ion exchange column studies at the small scale to improve the ability to predict full-scale behavior.

6.0 References

- ASME. 2000. *Quality Assurance Requirements for Nuclear Facility Applications*. NQA-1-2000, American Society of Mechanical Engineers, New York, New York.
- ASME. 2008. *Quality Assurance Requirements for Nuclear Facility Applications*. NQA-1-2008, American Society of Mechanical Engineers, New York, New York.
- ASME. 2009. *Addenda to ASME NQA-1-2008*. NQA-1a-2009, American Society of Mechanical Engineers, New York, New York.
- Bray, LA 1995. *Efficient Separations and Processing Crosscutting Program: Develop and Test Sorbents*. PNL-10750. Pacific Northwest Laboratory, Richland, Washington.
- Brown GN, LA Bray, CD Carlson, KJ Carson, JR DesChane, RJ Elovich, FV Hoopes, DE Kurath, LL Nenner, and PK Tanaka. 1996. *Comparison of Organic and Inorganic Ion Exchangers for Removal of Cesium and Strontium from Simulated and Actual Hanford 241-AW-101 DSSF Tank Waste*. PNNL-11120, Pacific Northwest National Laboratory, Richland, Washington.
- Buckingham J. 1967. *Waste Management Technical Manual*. ISO-100, Isochem, Incorporated. Richland, Washington.
- Campbell, EL, AM Rovira, F Colon-Cintron, D Boglajenko, TG Levitskaia, RA Peterson. 2019. *Characterization of Cs-Loaded CST Used for Treatment of Hanford Tank Waste in Support of Tank-Side Cesium Removal*. PNNL-28945, Rev. 0, RPT-TCT-005, Rev. 0, Pacific Northwest National Laboratory, Richland, Washington.
- Fiskum, SK, RA Peterson, HA Colburn, MR Smoot, MR Landon, KA Colosi and RA Wilson. 2019a. "Small- to large-scale comparisons of cesium ion exchange performance with spherical resorcinol formaldehyde resin." *Separation Science and Technology* **54**(12): 1922-1931.
- Fiskum SK, AM Rovira, JR Allred, HA Colburn, MR Smoot, AM Carney, TT Trang-Le, MG Cantaloub, EC Buck, and RA Peterson. 2019b. *Cesium Removal from Tank Waste Simulants Using Crystalline Silicotitanate at 12% and 100% TSCR Bed Heights*. PNNL-28527, Rev. 0; RPT-TCT-001, Rev. 0, Pacific Northwest National Laboratory, Richland, Washington.
- Fiskum SK, AM Rovira, HA Colburn, AM Carney, and RA Peterson. 2019c. *Cesium Ion Exchange Testing Using a Three-Column System with Crystalline Silicotitanate and Hanford Tank Waste 241-AP-107*. PNNL-28958, Rev. 0; RPT-DFTP-013, Rev. 0, Pacific Northwest National Laboratory, Richland, Washington.
- Fiskum SK, HA Colburn, RA Peterson, AM Rovira, and MR Smoot. 2018. *Cesium Ion Exchange Using Crystalline Silicotitanate with 5.6 M Sodium Simulant*. PNNL-27587, Rev. 0; RPT-DFTP-008, Rev. 0, Pacific Northwest National Laboratory, Richland, Washington.
- Harland, C. (1994). *Ion Exchange: Theory and Practice, 2nd Edition*. Cambridge, United Kingdom, The Royal Society of Chemistry.
- Helfferich, F. (1962). *Ion Exchange*. New York, New York, McGraw-Hill Book Company, Inc.

Hougan OA and WR Marshall, Jr. 1947. "Adsorption from a Fluid Stream Flowing Through a Stationary Granular Bed." *Chemical Engineering Progress* 43(4):197-208.

King WD. 2007. *Literature Reviews to Support Ion Exchange Technology Selection for Modular Salt Processing*. WSRC-STI-2007-00609, Washington Savannah Company, Aiken, South Carolina.

Klinkenberg A. 1994. "Numerical Evaluation of Equations Describing Transient Heat and Mass Transfer in Packed Solids." *Industrial and Engineering Chemistry* 40(10):1992.

Rovira, AM, SK Fiskum, JR Allred, JGH Geeting, HA Colburn, AM Carney, TT Trang-Le and RA Peterson. 2019. *Dead-End Filtration and Crystalline Silicotitanate Cesium Ion Exchange with Hanford Tank Waste AW-102*. PNNL-28783, Rev. 0, RPT-TCT-003, Rev. 0. Pacific Northwest National Laboratory. Richland, Washington.

Rovira, AM, SK Fiskum, HA Colburn, JR Allred, MR Smoot and RA Peterson. 2018. *Cesium Ion Exchange Testing Using Crystalline Silicotitanate with Hanford Tank Waste 241-AP-107*. PNNL-27706, RPT-DFTP-011, Rev. 0. Pacific Northwest National Laboratory. Richland, Washington.

Russell RL, PP Schonewill, and CA Burns. 2017. *Simulant Development for LAWPS Testing*. PNNL-26165, Rev. 0; RPT-LPIST-001, Rev. 0, Pacific Northwest National Laboratory, Richland, Washington.

Walker, Jr. JF, PA Taylor, RL Cummins, BS Evans, SD Heath, JD Hewitt, RD Hunt, HL Jennings, JA Kilby, DD Dee, S Lewis-Lambert, SA Richardson, and RF Utrera. 1998. *Cesium Removal Demonstration Utilizing Crystalline Silicotitanate Sorbent for Processing Melton Valley Storage Tank Supernate: Final Report*. ORNL/TM-13503, Oak Ridge National Laboratory, Oak Ridge, Tennessee.

Appendix A – Column Load Data

The raw Cs breakthrough data for processing 5.6 M Na simulant through <25 mesh and <35 mesh CST beds are provided in Table A.1. The feed displacement, water rinse, and final fluid expulsion raw data are provided in Table A.2. The raw data include the processed bed volumes (BVs) and corresponding ¹³⁷Cs concentrations in the collected samples, % C/C₀, and the decontamination factors (DFs). The <25 mesh CST (Purple column) test also includes the elapsed time (in days) for comparison to the on-line detection results.

Table A.1. Cs Breakthrough Results with <25 mesh and <35 mesh CST Lot 2002009604

<25 Mesh CST (Purple)					<35 Mesh CST (Green)			
BV	Elapsed Time, Days	¹³⁷ Cs, μCi/ mL	% C/C ₀	DF	BV	¹³⁷ Cs, μCi/ mL	% C/C ₀	DF
8.5	0.2	2.21E-6	2.54E-2	3.93E+3	10.6	2.76E-7	3.18E-3	3.14E+4
53.6	1.2	2.23E-6	2.57E-2	3.89E+3	47.6	9.13E-8	1.05E-3	9.51E+4
96.8	2.2	7.37E-7	8.48E-3	1.18E+4	90.4	<1.43E-7	<1.64E-3	>6.10E+4
142.1	3.2	3.23E-6	3.71E-2	2.69E+3	134.3	9.11E-8	1.05E-3	9.53E+4
185.3	4.1	1.01E-5	1.16E-1	8.61E+2	177.6	3.49E-7	4.02E-3	2.49E+4
228.5	5.1	2.41E-5	2.78E-1	3.60E+2	222.6	1.82E-6	2.10E-2	4.77E+3
268.8	6.0	5.61E-5	6.46E-1	1.55E+2	263.8	5.88E-6	6.77E-2	1.48E+3
314.8	7.1	1.05E-4	1.21E+0	8.26E+1	308.8	1.69E-5	1.94E-1	5.15E+2
356.4	8.0	1.80E-4	2.07E+0	4.82E+1	351.4	3.84E-5	4.42E-1	2.26E+2
399.5	9.0	2.93E-4	3.37E+0	2.97E+1	395.1	7.81E-5	8.99E-1	1.11E+2
441.1	10.0	4.19E-4	4.82E+0	2.07E+1	438.6	1.44E-4	1.66E+0	6.02E+1
483.8	11.0	6.15E-4	7.08E+0	1.41E+1	482.4	2.41E-4	2.77E+0	3.61E+1
526.3	11.9	8.31E-4	9.57E+0	1.04E+1	525.3	4.03E-4	4.64E+0	2.15E+1
569.0	12.9	1.02E-3	1.18E+1	8.48E+0	568.3	6.10E-4	7.03E+0	1.42E+1
614.8	13.9	1.31E-3	1.51E+1	6.62E+0	613.7	7.21E-4	8.30E+0	1.20E+1
658.4	14.9	1.66E-3	1.91E+1	5.23E+0	658.1	1.18E-3	1.36E+1	7.36E+0
708.8	15.8	2.07E-3	2.39E+1	4.19E+0	701.2	1.42E-3	1.64E+1	6.11E+0
755.5	16.8	2.42E-3	2.79E+1	3.59E+0	745.2	1.80E-3	2.07E+1	4.83E+0
799.3	17.8	2.75E-3	3.16E+1	3.16E+0	788.7	2.22E-3	2.55E+1	3.92E+0
844.6	18.8	3.04E-3	3.50E+1	2.86E+0	833.4	2.43E-3	2.80E+1	3.57E+0
883.7	19.7	3.61E-3	4.15E+1	2.41E+0	872.4	3.06E-3	3.53E+1	2.84E+0
925.9	20.6	3.79E-3	4.37E+1	2.29E+0	914.6	3.38E-3	3.90E+1	2.57E+0
970.7	21.6	4.03E-3	4.64E+1	2.15E+0	959.5	3.74E-3	4.30E+1	2.33E+0
1013.7	22.6	4.26E-3	4.91E+1	2.04E+0	1003.0	4.03E-3	4.64E+1	2.16E+0

BV = bed volume, 10 mL

DF = decontamination factor

C₀ = 8.69E-3 μCi ¹³⁷Cs/ mL, 6.00E-5 M Cs

Table A.2. Feed Displacement, Water Rinse, and Final Flush Results

<25 Mesh CST (Purple)				<35 Mesh CST (Green)			
BV	¹³⁷ Cs, μCi/ mL	% C/C ₀	DF	BV	¹³⁷ Cs, μCi/ mL	% C/C ₀	DF
Feed Displacement							
1014.6	4.63E-3	5.33E+1	1.88E+0	1003.9	4.57E-3	5.26E+1	1.90E+0
1015.6	4.71E-3	5.43E+1	1.84E+0	1004.8	4.47E-3	5.15E+1	1.94E+0
1016.6	3.16E-3	3.64E+1	2.75E+0	1005.8	3.96E-3	4.56E+1	2.19E+0
1017.6	7.98E-4	9.18E+0	1.09E+1	1006.7	1.33E-3	1.53E+1	6.56E+0
1018.7	5.40E-4	6.22E+0	1.61E+1	1007.6	5.91E-4	6.80E+0	1.47E+1
1019.6	4.68E-4	5.38E+0	1.86E+1	1008.6	4.66E-4	5.36E+0	1.87E+1
Water Rinse							
1021.7	3.25E-4	3.74E+0	2.67E+1	1010.6	2.97E-4	3.42E+0	2.92E+1
1023.6	1.37E-4	1.57E+0	6.36E+1	1012.5	1.43E-4	1.65E+0	6.05E+1
1025.7	2.49E-5	2.87E-1	3.49E+2	1014.5	2.63E-5	3.02E-1	3.31E+2
1027.6	1.38E-5	1.59E-1	6.29E+2	1016.4	1.48E-5	1.70E-1	5.88E+2
1029.6	1.12E-5	1.29E-1	7.76E+2	1018.4	9.48E-6	1.09E-1	9.17E+2
1031.8	9.09E-6	1.05E-1	9.56E+2	1020.5	8.52E-6	9.81E-2	1.02E+3
Final Argon Flush							
1035.7	2.67E-5	3.08E-1	3.25E+2	1022.3	6.68E-5	7.69E-1	1.30E+2

BV = bed volume, 10 mL
DF = decontamination factor
C₀ = 8.69E-3 μCi ¹³⁷Cs/ mL, 6.00E-5 M Cs

Appendix B – Particle Size Analysis

This appendix provides the particle size distribution (PSD) for the <25 mesh and <35 mesh, washed crystalline silicotitanate (CST). The PSDs were measured pre-sonication, during sonication, and post-sonication. Table B.1 provides a cross-reference for each sample, process condition, and figure identification where the results are shown.

Table B.1. Cross-Reference of PSD Samples, Process Conditions, and Appendix Figure

Sample Identification	Sieve Cut	Sonication Status	Figure
TI065-25PSD-2.1- Average	<25 mesh	Pre-sonication	B.1
TI065-25PSD-2.2- Average	<25 mesh	Sonicated	B.2
TI065-25PSD-2.3- Average	<25 mesh	Post-sonication	B.3
TI065-35PSD-1.1- Average	<35 mesh	Pre-sonication	B.4
TI065-35PSD-1.2 - Average	<35 mesh	Sonicated	B.5
TI065-35PSD-1.3 - Average	<35 mesh	Post-sonication	B.6

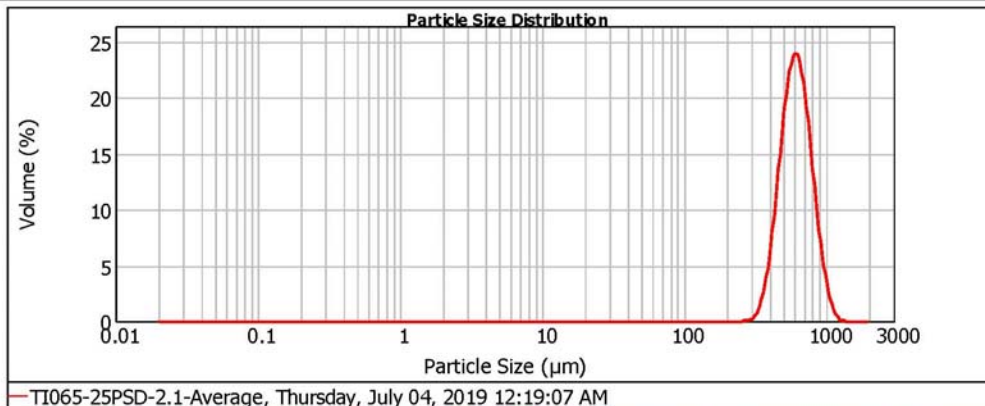


Result Analysis Report

Sample Name: TI065-25PSD-2.1-Average
Sample Source & type: D3M966
Sample bulk lot ref: Averaged
SOP Name:
Measured by: D3M966
Result Source: Averaged
Measured: Thursday, July 04, 2019 12:19:07 AM
Analysed: Thursday, July 04, 2019 12:19:09 AM

Particle Name: Zirconia av	Accessory Name: Hydro 2000G (A)	Analysis model: General purpose	Sensitivity: Normal
Particle RI: 2.165	Absorption: 1	Size range: 0.020 to 2000.000 um	Obscuration: 7.03 %
Dispersant Name: Water	Dispersant RI: 1.330	Weighted Residual: 1.999 %	Result Emulation: Off
Concentration: 0.6154 %Vol	Span : 0.642	Uniformity: 0.204	Result units: Volume
Specific Surface Area: 0.0101 m ² /g	Surface Weighted Mean D[3,2]: 594.200 um	Vol. Weighted Mean D[4,3]: 630.747 um	

d(0.1): 446.954 um d(0.5): 611.788 um d(0.9): 839.735 um



Size (µm)	Volume In %										
0.020	0.00	0.142	0.00	1.002	0.00	7.096	0.00	50.238	0.00	355.656	2.81
0.022	0.00	0.159	0.00	1.125	0.00	7.962	0.00	56.368	0.00	399.052	6.42
0.025	0.00	0.178	0.00	1.262	0.00	8.934	0.00	63.246	0.00	447.744	11.26
0.028	0.00	0.200	0.00	1.416	0.00	10.024	0.00	70.963	0.00	502.377	15.81
0.032	0.00	0.224	0.00	1.589	0.00	11.247	0.00	79.621	0.00	563.677	18.06
0.036	0.00	0.252	0.00	1.783	0.00	12.619	0.00	89.337	0.00	632.456	17.07
0.040	0.00	0.283	0.00	2.000	0.00	14.159	0.00	100.237	0.00	709.627	13.21
0.045	0.00	0.317	0.00	2.244	0.00	15.887	0.00	112.468	0.00	796.214	8.36
0.050	0.00	0.356	0.00	2.518	0.00	17.825	0.00	126.191	0.00	893.367	4.21
0.056	0.00	0.399	0.00	2.825	0.00	20.000	0.00	141.589	0.00	1002.374	1.58
0.063	0.00	0.448	0.00	3.170	0.00	22.440	0.00	158.866	0.00	1124.683	0.31
0.071	0.00	0.502	0.00	3.557	0.00	25.179	0.00	178.250	0.00	1261.915	0.00
0.080	0.00	0.564	0.00	3.991	0.00	28.251	0.00	200.000	0.00	1415.892	0.00
0.089	0.00	0.632	0.00	4.477	0.00	31.698	0.00	224.404	0.00	1588.656	0.00
0.100	0.00	0.710	0.00	5.024	0.00	35.566	0.00	251.785	0.00	1782.502	0.00
0.112	0.00	0.796	0.00	5.637	0.00	39.905	0.00	282.508	0.13	2000.000	0.00
0.126	0.00	0.893	0.00	6.325	0.00	44.774	0.00	316.979	0.13		
0.142	0.00	1.002	0.00	7.096	0.00	50.238	0.00	355.656	0.76		

Operator notes: CST lot #2002009604, Sieved -25 Mesh

Figure B.1. Pre-sonication, <25 mesh CST Lot 2002009604

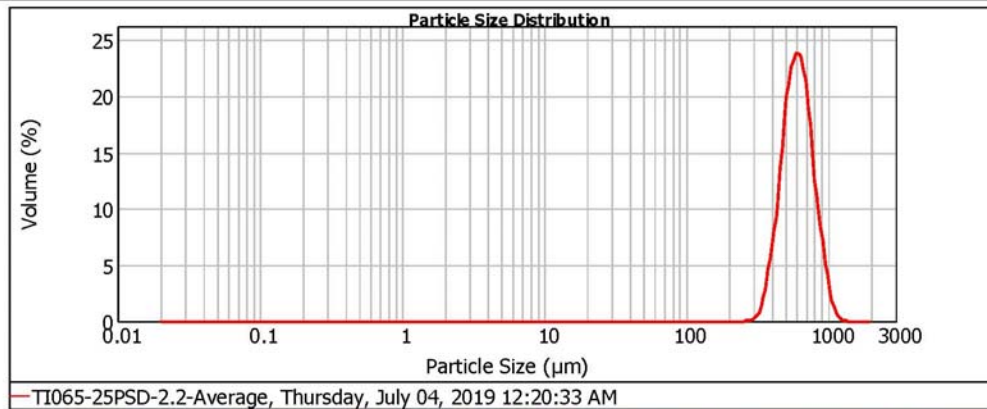


Result Analysis Report

Sample Name: TI065-25PSD-2.2-Average
Sample Source & type: D3M966
Sample bulk lot ref: Averaged
SOP Name:
Measured by: D3M966
Result Source: Averaged
Measured: Thursday, July 04, 2019 12:20:33 AM
Analysed: Thursday, July 04, 2019 12:20:35 AM

Particle Name: Zirconia av
Particle RI: 2.165
Dispersant Name: Water
Accessory Name: Hydro 2000G (A)
Absorption: 1
Dispersant RI: 1.330
Analysis model: General purpose
Size range: 0.020 to 2000.000 um
Weighted Residual: 1.954 %
Sensitivity: Normal
Obscuration: 9.68 %
Result Emulation: Off
Concentration: 0.8525 %Vol
Span : 0.648
Uniformity: 0.204
Result units: Volume
Specific Surface Area: 0.0102 m²/g
Surface Weighted Mean D[3,2]: 589.639 um
Vol. Weighted Mean D[4,3]: 625.936 um

d(0.1): 443.927 um d(0.5): 607.234 um d(0.9): 837.309 um



Size (µm)	Volume In %										
0.020	0.00	0.142	0.00	1.002	0.00	7.096	0.00	50.238	0.00	355.656	3.37
0.022	0.00	0.159	0.00	1.125	0.00	7.962	0.00	56.368	0.00	399.052	6.29
0.025	0.00	0.178	0.00	1.262	0.00	8.934	0.00	63.246	0.00	447.744	11.66
0.028	0.00	0.200	0.00	1.416	0.00	10.024	0.00	70.963	0.00	502.377	16.19
0.032	0.00	0.224	0.00	1.589	0.00	11.247	0.00	79.621	0.00	563.677	17.93
0.036	0.00	0.252	0.00	1.783	0.00	12.619	0.00	89.337	0.00	632.456	17.07
0.040	0.00	0.283	0.00	2.000	0.00	14.159	0.00	100.237	0.00	709.627	12.91
0.045	0.00	0.317	0.00	2.244	0.00	15.887	0.00	112.468	0.00	796.214	7.67
0.050	0.00	0.356	0.00	2.518	0.00	17.825	0.00	126.191	0.00	893.367	4.36
0.056	0.00	0.399	0.00	2.825	0.00	20.000	0.00	141.589	0.00	1002.374	1.33
0.063	0.00	0.448	0.00	3.170	0.00	22.440	0.00	158.866	0.00	1124.683	0.28
0.071	0.00	0.502	0.00	3.557	0.00	25.179	0.00	178.250	0.00	1261.915	0.00
0.080	0.00	0.564	0.00	3.991	0.00	28.251	0.00	200.000	0.00	1415.892	0.00
0.089	0.00	0.632	0.00	4.477	0.00	31.698	0.00	224.404	0.00	1588.656	0.00
0.100	0.00	0.710	0.00	5.024	0.00	35.566	0.00	251.785	0.00	1782.502	0.00
0.112	0.00	0.796	0.00	5.637	0.00	39.905	0.00	282.508	0.15	2000.000	0.00
0.126	0.00	0.893	0.00	6.325	0.00	44.774	0.00	316.979	0.15		
0.142	0.00	1.002	0.00	7.096	0.00	50.238	0.00	355.656	0.78		

Operator notes: CST lot #2002009604, Sieved -25 Mesh

Figure B.2. Sonicated, <25 mesh CST Lot 2002009604

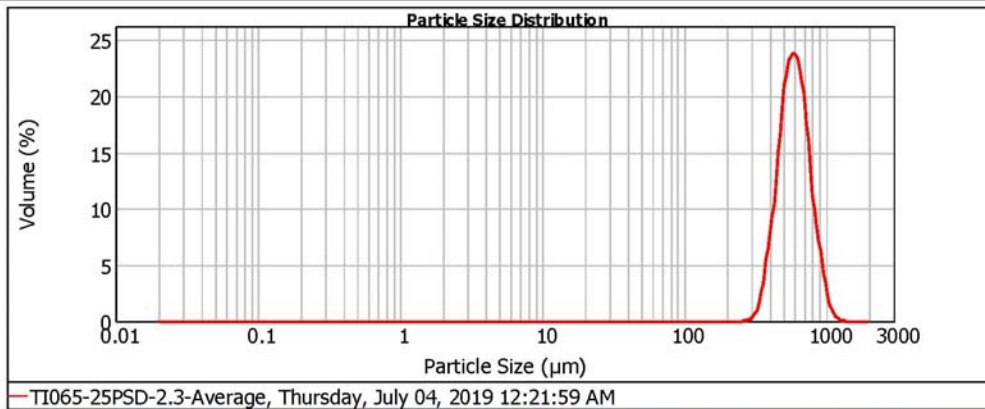


Result Analysis Report

Sample Name: TI065-25PSD-2.3-Average
Sample Source & type: D3M966
Sample bulk lot ref: Averaged
SOP Name:
Measured by: D3M966
Result Source: Averaged
Measured: Thursday, July 04, 2019 12:21:59 AM
Analysed: Thursday, July 04, 2019 12:22:00 AM

Particle Name: Zirconia av
Particle RI: 2.165
Dispersant Name: Water
Accessory Name: Hydro 2000G (A)
Absorption: 1
Dispersant RI: 1.330
Analysis model: General purpose
Size range: 0.020 to 2000.000 um
Weighted Residual: 2.086 %
Sensitivity: Normal
Obscuration: 11.53 %
Result Emulation: Off
Concentration: 1.0033 %Vol
Span : 0.646
Uniformity: 0.205
Result units: Volume
Specific Surface Area: 0.0104 m²/g
Surface Weighted Mean D[3,2]: 576.532 um
Vol. Weighted Mean D[4,3]: 611.994 um

d(0.1): 432.830 um d(0.5): 593.052 um d(0.9): 816.048 um



Size (µm)	Volume In %										
0.020	0.00	0.142	0.00	1.002	0.00	7.096	0.00	50.238	0.00	355.656	3.98
0.022	0.00	0.159	0.00	1.125	0.00	7.962	0.00	56.368	0.00	399.052	7.20
0.025	0.00	0.178	0.00	1.262	0.00	8.934	0.00	63.246	0.00	447.744	12.71
0.028	0.00	0.200	0.00	1.416	0.00	10.024	0.00	70.963	0.00	502.377	16.92
0.032	0.00	0.224	0.00	1.589	0.00	11.247	0.00	79.621	0.00	563.677	17.98
0.036	0.00	0.252	0.00	1.783	0.00	12.619	0.00	89.337	0.00	632.456	16.43
0.040	0.00	0.283	0.00	2.000	0.00	14.159	0.00	100.237	0.00	709.627	11.89
0.045	0.00	0.317	0.00	2.244	0.00	15.887	0.00	112.468	0.00	796.214	6.72
0.050	0.00	0.356	0.00	2.518	0.00	17.825	0.00	126.191	0.00	893.367	3.69
0.056	0.00	0.399	0.00	2.825	0.00	20.000	0.00	141.589	0.00	1002.374	1.03
0.063	0.00	0.448	0.00	3.170	0.00	22.440	0.00	158.866	0.00	1124.683	0.23
0.071	0.00	0.502	0.00	3.557	0.00	25.179	0.00	178.250	0.00	1261.915	0.00
0.080	0.00	0.564	0.00	3.991	0.00	28.251	0.00	200.000	0.00	1415.892	0.00
0.089	0.00	0.632	0.00	4.477	0.00	31.698	0.00	224.404	0.00	1588.656	0.00
0.100	0.00	0.710	0.00	5.024	0.00	35.566	0.00	251.785	0.00	1782.502	0.00
0.112	0.00	0.796	0.00	5.637	0.00	39.905	0.00	282.508	0.21	2000.000	0.00
0.126	0.00	0.893	0.00	6.325	0.00	44.774	0.00	316.979	0.00		
0.142	0.00	1.002	0.00	7.096	0.00	50.238	0.00	355.656	1.02		

Operator notes: CST lot #2002009604, Sieved -25 Mesh

Figure B.3. Post-sonication, <25 mesh CST Lot 2002009604

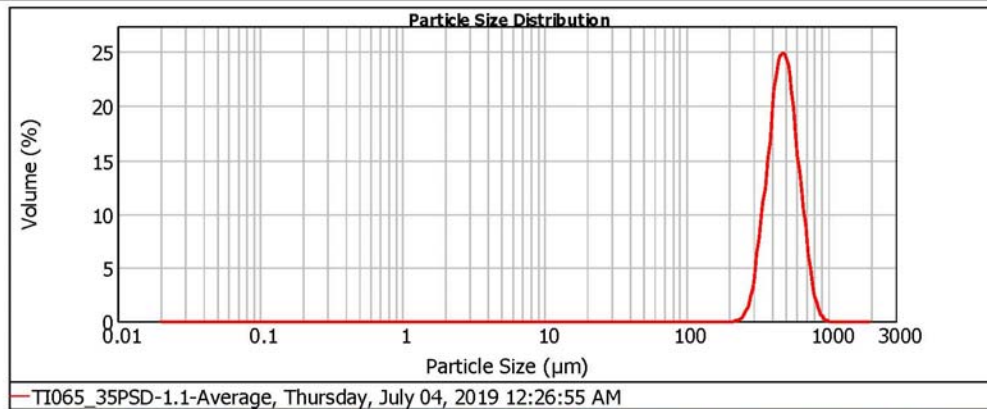


Result Analysis Report

Sample Name: TI065_35PSD-1.1-Average
SOP Name:
Measured: Thursday, July 04, 2019 12:26:55 AM
Sample Source & type: D3M966
Measured by: D3M966
Analysed: Thursday, July 04, 2019 12:26:56 AM
Sample bulk lot ref: Averaged
Result Source: Averaged

Particle Name: Zirconia av	Accessory Name: Hydro 2000G (A)	Analysis model: General purpose	Sensitivity: Normal
Particle RI: 2.165	Absorption: 1	Size range: 0.020 to 2000.000 um	Obscuration: 6.84 %
Dispersant Name: Water	Dispersant RI: 1.330	Weighted Residual: 1.766 %	Result Emulation: Off
Concentration: 0.4704 %Vol	Span : 0.625	Uniformity: 0.19	Result units: Volume
Specific Surface Area: 0.0128 m ² /g	Surface Weighted Mean D[3,2]: 467.645 um	Vol. Weighted Mean D[4,3]: 494.057 um	

d(0.1): 352.986 um d(0.5): 480.989 um d(0.9): 653.468 um



Size (µm)	Volume In %										
0.020	0.00	0.142	0.00	1.002	0.00	7.096	0.00	50.238	0.00	355.656	10.95
0.022	0.00	0.159	0.00	1.125	0.00	7.962	0.00	56.368	0.00	399.052	16.85
0.025	0.00	0.178	0.00	1.262	0.00	8.934	0.00	63.246	0.00	447.744	18.73
0.028	0.00	0.200	0.00	1.416	0.00	10.024	0.00	70.963	0.00	502.377	17.73
0.032	0.00	0.224	0.00	1.589	0.00	11.247	0.00	79.621	0.00	563.677	12.32
0.036	0.00	0.252	0.00	1.783	0.00	12.619	0.00	89.337	0.00	632.456	8.34
0.040	0.00	0.283	0.00	2.000	0.00	14.159	0.00	100.237	0.00	709.627	3.39
0.045	0.00	0.317	0.00	2.244	0.00	15.887	0.00	112.468	0.00	796.214	1.01
0.050	0.00	0.356	0.00	2.518	0.00	17.825	0.00	126.191	0.00	893.367	0.08
0.056	0.00	0.399	0.00	2.825	0.00	20.000	0.00	141.589	0.00	1002.374	0.00
0.063	0.00	0.448	0.00	3.170	0.00	22.440	0.00	158.866	0.00	1124.683	0.00
0.071	0.00	0.502	0.00	3.557	0.00	25.179	0.00	178.250	0.00	1261.915	0.00
0.080	0.00	0.564	0.00	3.991	0.00	28.251	0.00	200.000	0.00	1415.892	0.00
0.089	0.00	0.632	0.00	4.477	0.00	31.698	0.00	224.404	0.08	1588.656	0.00
0.100	0.00	0.710	0.00	5.024	0.00	35.566	0.00	251.785	0.71	1782.502	0.00
0.112	0.00	0.796	0.00	5.637	0.00	39.905	0.00	282.508	2.65	2000.000	0.00
0.126	0.00	0.893	0.00	6.325	0.00	44.774	0.00	316.979	7.16		
0.142	0.00	1.002	0.00	7.096	0.00	50.238	0.00	355.656			

Operator notes: CST lot #2002009604, Sieved -35 Mesh

Figure B.4. Pre-sonication, <35 mesh CST Lot 2002009604

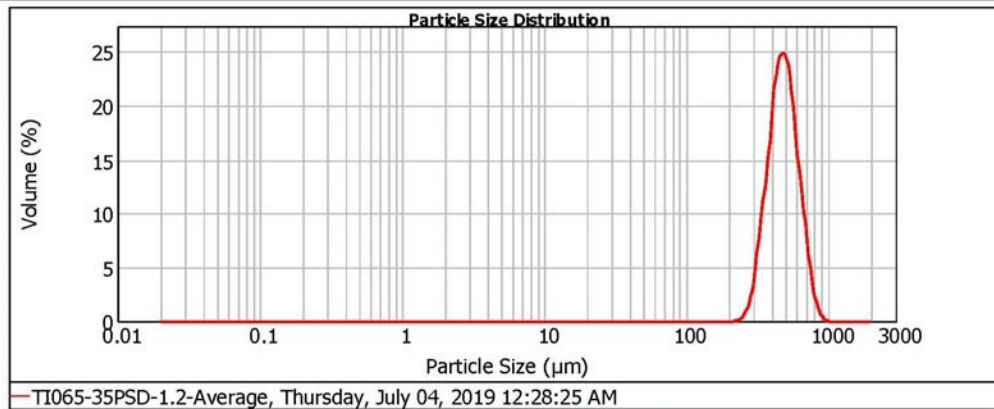


Result Analysis Report

Sample Name: TI065-35PSD-1.2-Average
Sample Source & type: D3M966
Sample bulk lot ref: Averaged
SOP Name:
Measured by: D3M966
Result Source: Averaged
Measured: Thursday, July 04, 2019 12:28:25 AM
Analysed: Thursday, July 04, 2019 12:28:27 AM

Particle Name: Zirconia av	Accessory Name: Hydro 2000G (A)	Analysis model: General purpose	Sensitivity: Normal
Particle RI: 2.165	Absorption: 1	Size range: 0.020 to 2000.000 um	Obscuration: 9.45 %
Dispersant Name: Water	Dispersant RI: 1.330	Weighted Residual: 1.708 %	Result Emulation: Off
Concentration: 0.6589 %Vol	Span : 0.626	Uniformity: 0.19	Result units: Volume
Specific Surface Area: 0.0128 m ² /g	Surface Weighted Mean D[3,2]: 467.345 um	Vol. Weighted Mean D[4,3]: 493.846 um	

d(0.1): 352.624 um d(0.5): 480.720 um d(0.9): 653.497 um



Size (µm)	Volume In %										
0.020	0.00	0.142	0.00	1.002	0.00	7.096	0.00	50.238	0.00	355.656	10.98
0.022	0.00	0.159	0.00	1.125	0.00	7.962	0.00	56.368	0.00	399.052	16.84
0.025	0.00	0.178	0.00	1.262	0.00	8.934	0.00	63.246	0.00	447.744	18.70
0.028	0.00	0.200	0.00	1.416	0.00	10.024	0.00	70.963	0.00	502.377	17.68
0.032	0.00	0.224	0.00	1.589	0.00	11.247	0.00	79.621	0.00	563.677	12.29
0.036	0.00	0.252	0.00	1.783	0.00	12.619	0.00	89.337	0.00	632.456	8.32
0.040	0.00	0.283	0.00	2.000	0.00	14.159	0.00	100.237	0.00	709.627	3.40
0.045	0.00	0.317	0.00	2.244	0.00	15.887	0.00	112.468	0.00	796.214	1.02
0.050	0.00	0.356	0.00	2.518	0.00	17.825	0.00	126.191	0.00	893.367	0.09
0.056	0.00	0.399	0.00	2.825	0.00	20.000	0.00	141.589	0.00	1002.374	0.00
0.063	0.00	0.448	0.00	3.170	0.00	22.440	0.00	158.866	0.00	1124.683	0.00
0.071	0.00	0.502	0.00	3.557	0.00	25.179	0.00	178.250	0.00	1261.915	0.00
0.080	0.00	0.564	0.00	3.991	0.00	28.251	0.00	200.000	0.00	1415.892	0.00
0.089	0.00	0.632	0.00	4.477	0.00	31.698	0.00	224.404	0.08	1588.656	0.00
0.100	0.00	0.710	0.00	5.024	0.00	35.566	0.00	251.785	0.73	1782.502	0.00
0.112	0.00	0.796	0.00	5.637	0.00	39.905	0.00	282.508	2.67	2000.000	0.00
0.126	0.00	0.893	0.00	6.325	0.00	44.774	0.00	316.979	7.19		
0.142	0.00	1.002	0.00	7.096	0.00	50.238	0.00	355.656			

Operator notes: CST lot #2002009604, Sieved -35 Mesh

Figure B.5. Sonicated, <35 mesh CST Lot 2002009604

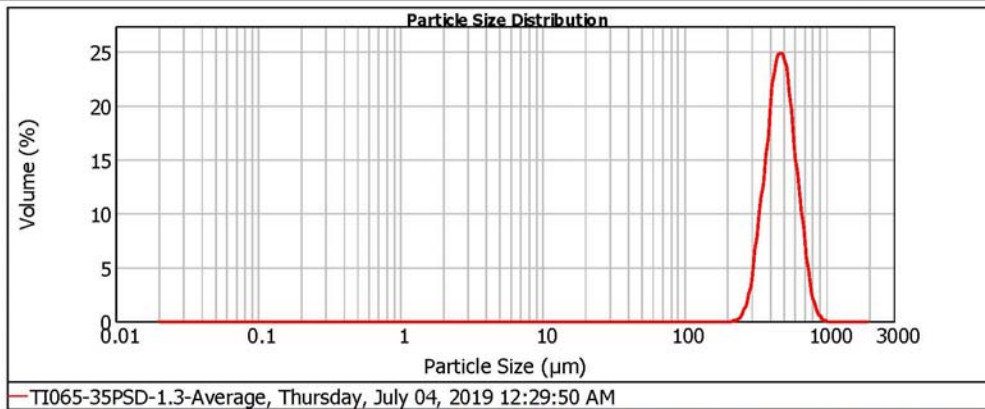


Result Analysis Report

Sample Name: TI065-35PSD-1.3-Average
Sample Source & type: D3M966
Sample bulk lot ref: Averaged
SOP Name:
Measured by: D3M966
Result Source: Averaged
Measured: Thursday, July 04, 2019 12:29:50 AM
Analysed: Thursday, July 04, 2019 12:29:52 AM

Particle Name: Zirconia av
Particle RI: 2.165
Dispersant Name: Water
Accessory Name: Hydro 2000G (A)
Absorption: 1
Dispersant RI: 1.330
Analysis model: General purpose
Size range: 0.020 to 2000.000 um
Weighted Residual: 1.635 %
Sensitivity: Normal
Obscuration: 11.19 %
Result Emulation: Off
Concentration: 0.7835 %Vol
Span : 0.626
Uniformity: 0.189
Result units: Volume
Specific Surface Area: 0.0129 m²/g
Surface Weighted Mean D[3,2]: 465.183 um
Vol. Weighted Mean D[4,3]: 491.581 um

d(0.1): 351.045 um d(0.5): 478.547 um d(0.9): 650.718 um



Size (µm)	Volume In %										
0.020	0.00	0.142	0.00	1.002	0.00	7.096	0.00	50.238	0.00	355.656	11.19
0.022	0.00	0.159	0.00	1.125	0.00	7.962	0.00	56.368	0.00	399.052	16.98
0.025	0.00	0.178	0.00	1.262	0.00	8.934	0.00	63.246	0.00	447.744	18.71
0.028	0.00	0.200	0.00	1.416	0.00	10.024	0.00	70.963	0.00	502.377	17.57
0.032	0.00	0.224	0.00	1.589	0.00	11.247	0.00	79.621	0.00	563.677	12.09
0.036	0.00	0.252	0.00	1.783	0.00	12.619	0.00	89.337	0.00	632.456	8.13
0.040	0.00	0.283	0.00	2.000	0.00	14.159	0.00	100.237	0.00	709.627	3.26
0.045	0.00	0.317	0.00	2.244	0.00	15.887	0.00	112.468	0.00	796.214	0.95
0.050	0.00	0.356	0.00	2.518	0.00	17.825	0.00	126.191	0.00	893.367	0.08
0.056	0.00	0.399	0.00	2.825	0.00	20.000	0.00	141.589	0.00	1002.374	0.00
0.063	0.00	0.448	0.00	3.170	0.00	22.440	0.00	158.866	0.00	1124.683	0.00
0.071	0.00	0.502	0.00	3.557	0.00	25.179	0.00	178.250	0.00	1261.915	0.00
0.080	0.00	0.564	0.00	3.991	0.00	28.251	0.00	200.000	0.00	1415.892	0.00
0.089	0.00	0.632	0.00	4.477	0.00	31.698	0.00	224.404	0.09	1588.656	0.00
0.100	0.00	0.710	0.00	5.024	0.00	35.566	0.00	251.785	0.79	1782.502	0.00
0.112	0.00	0.796	0.00	5.637	0.00	39.905	0.00	282.508	2.80	2000.000	0.00
0.126	0.00	0.893	0.00	6.325	0.00	44.774	0.00	316.979	2.80		
0.142	0.00	1.002	0.00	7.096	0.00	50.238	0.00	355.656	7.37		

Operator notes: CST lot #2002009604, Sieved -35 Mesh

Figure B.6. Post-sonication, <35 mesh CST Lot 2002009604

Appendix C – On-line Gamma Analysis

This appendix provides details of the on-line gamma detection system and results for the <25-mesh crystalline silicotitanate (CST) (Purple system) test. The information provided herein is for information only (FIO). The system utilization and data analysis were not conducted under the controls of the QA program described in Section 2.0 of this report.

C.1 Experimental

The effluent from the <25-mesh CST (Purple system) was monitored for ^{137}Cs activity using two cerium doped lanthanum-bromide ($\text{LaBr}_3(\text{Ce})$) detectors (LaBr) and a “flow-through” thallium-doped sodium-iodide ($\text{NaI}(\text{Tl})$) detector (NaI). The multiple detectors were set up to demonstrate in-line near real-time monitoring of the ion exchange column performance using commercial off-the-shelf equipment and software, and to explore more recent developments in list-mode data acquisition and data management. Additionally, the setup was chosen to explore the potential equilibrium/dis-equilibrium state of ^{137}Cs and $^{137\text{m}}\text{Ba}$ in the ion exchange effluent.

The LaBr detectors were Saint Gobain BriLance-380 detectors. Each detector was coupled to a 14-pin photomultiplier tube (PMT) base providing high-voltage input (HV), signal out and a manual gain adjustment. An Ortec 556H desktop high-voltage power supply provided HV to each LaBr detector, while the detector outputs were routed to separate channels on a CAEN DT5781 quad digital multichannel analyzer (MCA; digitizer). The digitizer was configured and controlled using CAENs MC2 Analyzer software (v 2.1.2.0) connected to a Win7 personal computer (PC).

The NaI “flow-through” detector was a Bicon 3x3 NaI detector originally from an automated gamma counter. The detector was nominally 3 in. x 3 in. NaI (7.6 cm diameter x 7.6 cm tall) with a 1.27-cm diameter penetration through the crystal, perpendicular to the crystal and PMT axis. The detector was coupled to a Canberra Osprey digital tube base for HV bias and acquisition. Detector parameters and data acquisition were performed on a Win7 PC (same PC as the CAEN) using Canberra’s Genie 2K gamma spectroscopy suite (V3.4). Table C.1 provides the complete listing of the acquisition hardware and signal processing components.

Table C.1. In-line Gamma Analysis Equipment List

Detector	Model	PMT Base	HV	MCA/Pulse Processing	Software
LaBr ₃ (Ce)-1	Saint Gobain BriLance 38S 38; SN A2400	Rexon RB-14; SN 15351-3	Ortec 556H; SN 18106985	CAEN DT5781 quad digital MCA digitizer; SN 1736	CAEN MC2 Analyzer v2.1.2.0
LaBr ₃ (Ce)-2	Saint Gobain BriLance 38S 38; SN A2403	Rexon RB-14; SN 15351-2	Ortec 556H; SN 18106985	CAEN DT5781 quad digital MCA digitizer; SN 1736	CAEN MC2 Analyzer v2.1.2.0
NaI(Tl)	Bicon 3M3W 3/3-X	Canberra Osprey DTB; SN 13002685	Canberra Osprey DTB; SN 13002685	Canberra Osprey DTB; SN 13002685	Canberra G2K v3.4

The LaBr detectors were each surrounded by tight-fitting lead shields, providing approximately 2.5 cm of lead thickness around each detector. Detector shielding was installed in two pieces (top and bottom) that were constructed with a channel allowing the effluent flow tube to enter and exit the shield and cross perpendicular to the face of the two LaBr detectors at a distance of less than 0.5 cm. Additional shielding in the form of standard lead bricks (nominally 10 cm x 20 cm x 5 cm – width x length x depth) was placed around the individual detector shields as needed to provide a nominal 12.5 cm of shielding between the detectors and potential radiation sources originating from the experimental setup (ion exchange column, the simulant supply carboy, the effluent collection container – see the in-line detection schematic, Figure C.1).

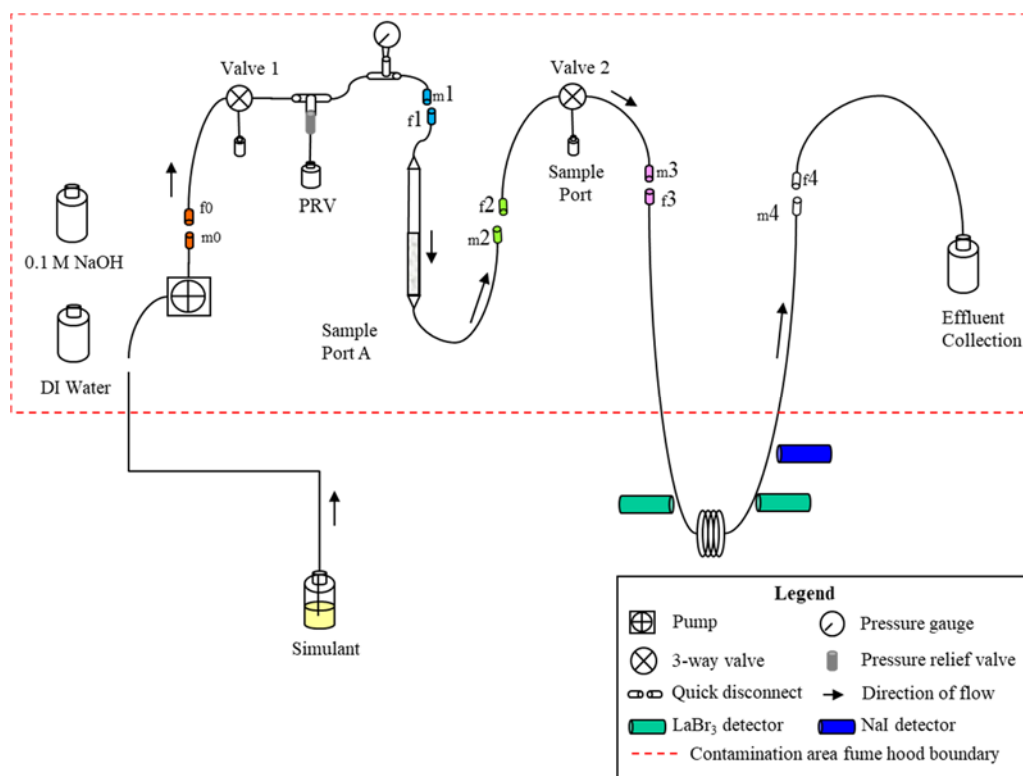


Figure C.1. System Schematic

The NaI flow-through detector was shielded with a detector-specific machined shield providing over 5 cm of lead around the detector and with the needed penetrations to allow effluent tubing to pass through the shield and detector. The detector and shield were oriented so flow traveled vertically through the detector, coming from below the detector/shield and exiting at the top of the detector/shield. As with the LaBr detectors, additional lead bricks were placed around the NaI detector shield to minimize background intrusion on the detector.

As depicted in Figure C.1, flow into the detection system started after ion exchange effluent passed through quick disconnects $m3/f3$. There was an effective 3.1-mL mixing chamber below the CST bed support screen before fluid flow entered the 0.16-cm-diameter tubing. Effluent traveled ~1.5 m to quick disconnect $m3/f3$, then an additional ~1 m before going past the LaBr-1 detector. Effluent then exited into a delay coil, which consisted of six 25-cm-diameter “loops” of flow tube providing nearly 480 linear cm of travel prior to running past LaBr-2, the flow went almost immediately

into the NaI flow-through detector before leaving the inline system and returning to the fume hood for bulk effluent collection.

The effluent traveled throughout the in-line measurement system in a contiguous “tube-within-tube” configuration. The inner tube consisted of 0.16-cm-inside-diameter (ID) polyethylene tubing that was in turn fed through an outer 0.75-cm-ID nylon tubing. Connection to the ion exchange system was made with the inner tube while the outer tube provided protection to the inner tube from abrasion and pinching as it was threaded through the detector shielding penetrations, as well as containment in the unlikely event of breaching the inner tube or a leaking connection at the $m3/f3$ or $m4/f4$ fittings.

Linear flow through the system was slightly more than 15 cm/min at a nominal volumetric flowrate of 0.305 mL/min. At that same volumetric flowrate, the delay coil provided approximately 30 min delay between measuring an effluent “slug” at LaBr-1 detector and then LaBr-2.

The detectors, shielding, electronics, and PC were assembled on a wheeled, steel cart rated at 2000 lb. A 0.61-cm-thick aluminum plate was placed on the cart to minimize deflection of the cart’s 0.32-cm-thick steel surface from the weight of lead shielding. The in-line monitoring system weighed approximately 1200 lb. Assembling the detectors and shielding required threading the tubing through the system as it was assembled into the final configuration. Approximately 100 cm of the tube-within-tube was available at both ends of the system for the connecting of the inline detection system to the ion exchange system (connections $m3/f3$ and $m4/f4$, Figure C.1).

C.2 Data Acquisition and Analysis

The LaBr detectors were controlled via the CAEN digitizer and MC2 Analyzer software configured for list-mode acquisition. The list-mode data acquisition produces time stamped, event-by-event interaction data from the detector. The CAEN digitizers use binary format to minimize data size and transfer time as time-stamped data for each detector is transferred directly to the PC hard drive. Data analysis is performed offline using a ROOT data processing package to recreate detector response in counts per second (cps) as a function of acquisition duration.

The NaI flow-through detector data were acquired as distinct spectra for a given count time (real time) over the duration of the experiment. Count times varied from 5 h at the start of effluent flow when ^{137}Cs was expected to be low, to 1 h as the effluent radioactivity increased. Acquisition spectra were automatically saved and new counts started to provide near-continuous effluent monitoring with minimal operator interaction. The gross, background, and net count rate (in cps) were determined for a fixed region of interest (ROI), channel 380 to 543, in each spectrum that included the ^{137}Cs 661 keV gamma line, and for a time corresponding to the mid-point of the data acquisition (e.g., a 1-h live time acquisition started at 13:00 was plotted as 13:30).

Figure C.2 is a photograph of the in-line detection system. Detector LaBr-1 is at the right side of the cart and detector LaBr-2 is in the middle of the cart, below the keyboard/plexiglass sheet. The NaI flow-through detector is at the far left. The delay coil is not visible but is situated in between LaBr-2 and the video monitor. Flow into the system started at the right with the white tube going into the lead brick and exited through the top of the NaI detector and routed back to the fume hood.

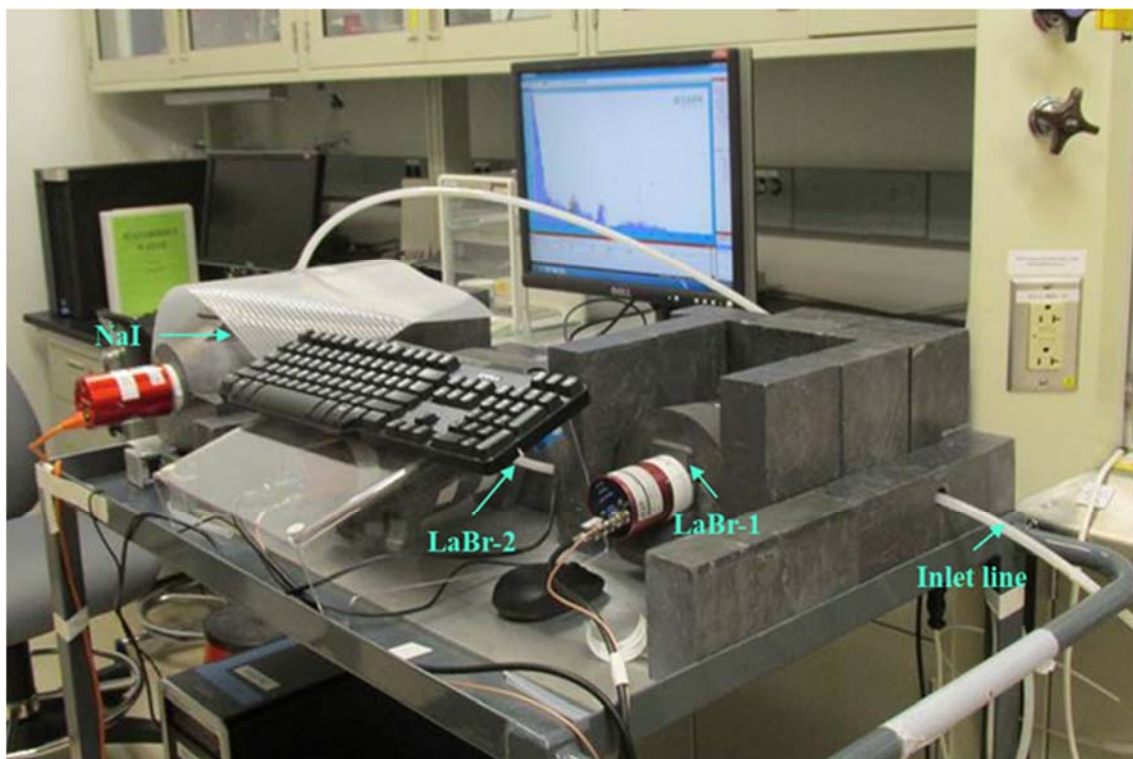


Figure C.2. Near Final Assembly of the In-Line Effluent Measurement System prior to Connection to the Ion Exchange System

C.3 Results

This section describes the results obtained from both the LaBr and NaI on-line detectors.

C.3.1 LaBr and List-Mode Acquisition

The dual LaBr detection system suffered from unreliable data acquisition and storage issues throughout the experiment. While the data transfer rates were small (~30 kB per minute) and total data file sizes modest (~50 MB for both detectors after 24 h of operation), the CAEN digitizer and MC2 Analyzer software frequently seized, stopping data acquisition. The lockup and data loss appeared related to PC demands, particularly while data (CAEN or Canberra) were transferred from the PC hard drive to an external drive for processing. Despite the data drop-outs, there were intervals of continuous list-mode data acquisition as shown in Figure C.3.

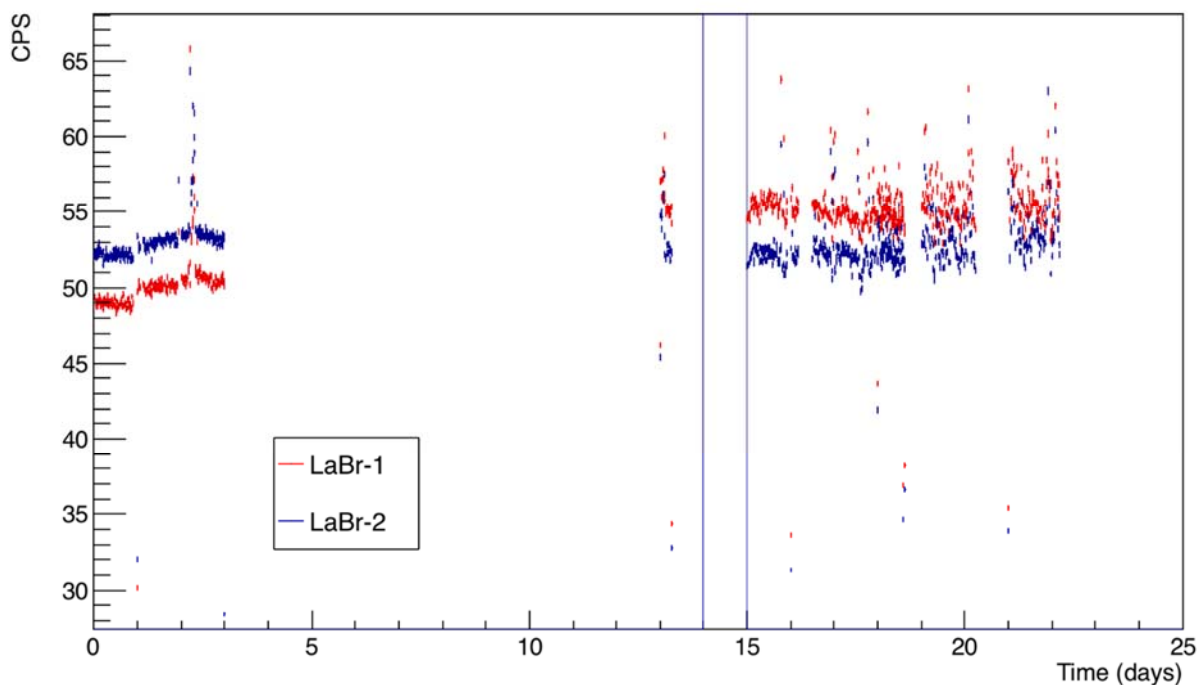


Figure C.3. Count-Rates Observed from the LaBr Detectors during the Acquisition Run. Data drop-outs are observed as the acquisition system was not reliable during the operation.

The low-effluent ^{137}Cs gamma spectra were not easily observed due to the high background inherent to LaBr detectors. Using lower background detectors (like NaI), eliminating the mixing volume below the CST bed, and shortening the distance from the base of the column to the detectors in future measurements will likely provide better insight into the dis-equilibrium between the parent and daughter as a function of column loading.

Figure C.4 depicts the time-series spectra that may be generated and re-evaluated using variable time-bin widths. Features observed in this waterfall plot are the traditional background features associated with LaBr detectors. These background features interfered with the observation and quantification of the ^{137}Cs peak (note that in this case the entire spectral range was integrated for ^{137}Cs).

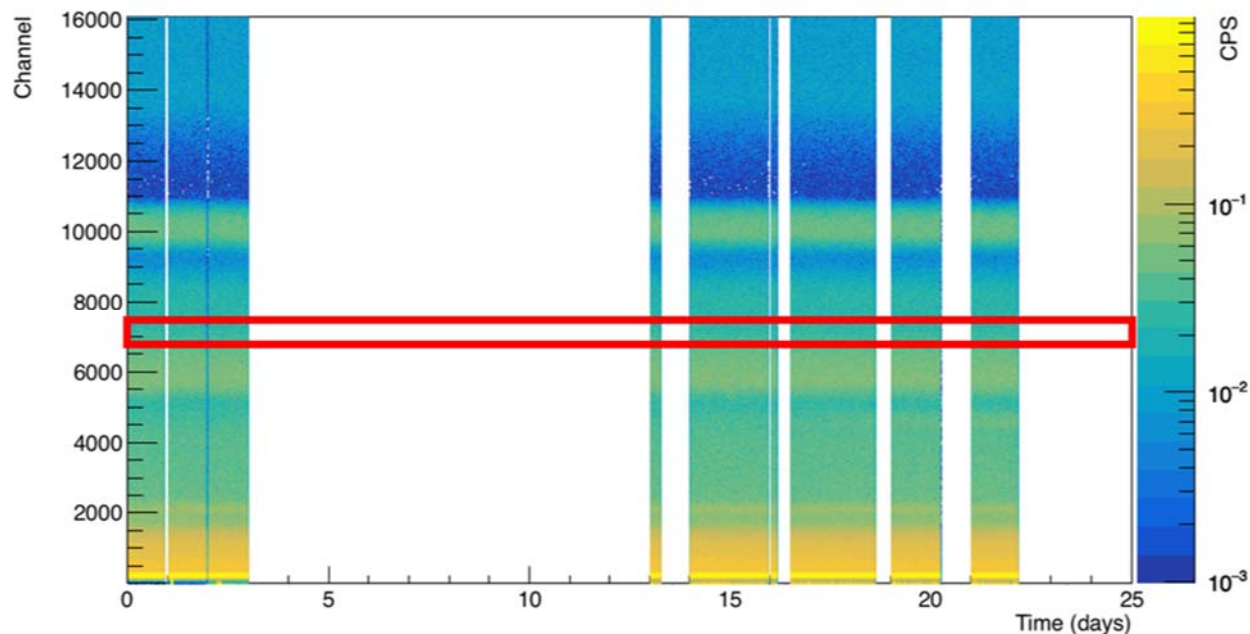


Figure C.4. Water-Fall Plot Recreated from Time-Stamped List Mode Data

The two LaBr detectors were set up with a 30-min delay between the segment of effluent passing in front of LaBr-1 and then LaBr-2 detector (flow rate of 0.308 mL/min and superficial velocity of 15 cm/min). ^{137}Cs decays by beta emission to an excited state of ^{137}Ba ($^{137\text{m}}\text{Ba}$). This excited state returns to ground state by emission of a 661-keV gamma ray with a 2.55-min half-life. Unperturbed, a $^{137}\text{Cs}/^{137\text{m}}\text{Ba}$ secular equilibrium is achieved after 15 min. Depending on flowrate through the ion exchange column, the exchange potential for ^{137}Cs and $^{137\text{m}}\text{Ba}$, and mixing time in the chamber below the bed, the parent and daughter may not be in equilibrium at the column effluent, such that the $^{137\text{m}}\text{Ba}$ activity could be more, or less, than the ^{137}Cs activity. The delay coil provided ample time for secular equilibrium to be achieved between ^{137}Cs and $^{137\text{m}}\text{Ba}$ prior to measurement at LaBr-2. Even if LaBr detector performance was perfect, LaBr-1 was likely situated too far downstream, 8 min (not incorporating the mixing chamber below the CST bed), from the ion exchange bed effluent to accurately assess the equilibrium status.

C.3.2 NaI Flow-through Detector Data Acquisition

The NaI detector had nearly 100% availability during the experiment, the only exception being when acquisition count time was adjusted from 5 h to 1 h real time, and at several times when automatic acquisition was reset within the G2K software. Figure C.5 plots the NaI detector ROI net count rate as a function of the elapsed time from the start of flow through the in-line system until completion of ion exchange flow and a subsequent in-line system flush.

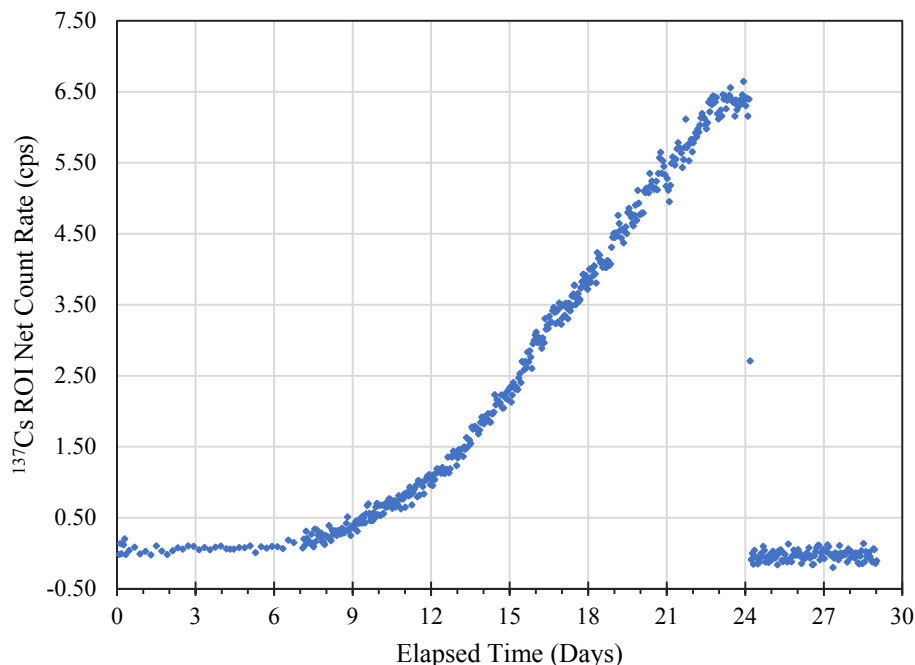


Figure C.5. Net NaI Flow-Through Detector Net Count Rate for the ^{137}Cs ROI as a Function of Elapsed Measurement Time (days) for the Duration of Ion Exchange Flow and the Post Experiment System Flush

While the system was not calibrated to provide direct ^{137}Cs activity, the net detector cps provided an excellent trace of the effluent activity with time. No attempt was made to adjust the data to account for the 30-45 min of “no-flow” each day as a 10-mL effluent sample was collected for ^{137}Cs analysis, or for changes in volumetric flowrate. Thus, the elapsed time scale shown in Figure C.5 is not a direct representation of the total volume flowing through the system. One-hour counts were obtained at the beginning of the flow, but then changed to 5-h per count from day 1 to day 7, after which count times returned to 1 h. The overall curve shape met expectations, though the curvature appeared to change at or about day 16 as seen in Figure C.5, with an inflection point at day 16 and the subsequent data showing a more linear trend. This day-16 change corresponded to the transient change in column flowrate to 0.358 mL/min.

The NaI flow-through detector net count rate returned to background (i.e., ~ 0 cps) within 1 day of system flushing. While not obvious from the net detector count rate data, the end of experiment system background was lower than system background at the beginning of the experiment as shown in Figure C.6, which plots the 5-h average gross count rates for the ^{137}Cs ROI. One reason for this is a known change in the laboratory background. Also, as shown in Figure C.6, at about day 11, there was a distinct step change in the gross count rate that corresponded to removal of radioactive waste from the laboratory space. This points out one deficiency of the system setup in that detector shielding was focused primarily on the radiation sources related to the experiment itself (e.g., delay coil, simulant reservoir) with the additional shield bricks stacked toward the front of the detector(s), rather than all the way around the detector. This failed to account for background radiation in the room, primarily the radioactive waste storage container that was nearest the NaI detector.

The gradual “steps” of the detector gross count rate for the first 3 days of flow also suggested decreasing ^{137}Cs count rate; this was consistent with the ^{137}Cs concentration decrease observed from discrete sample collection.

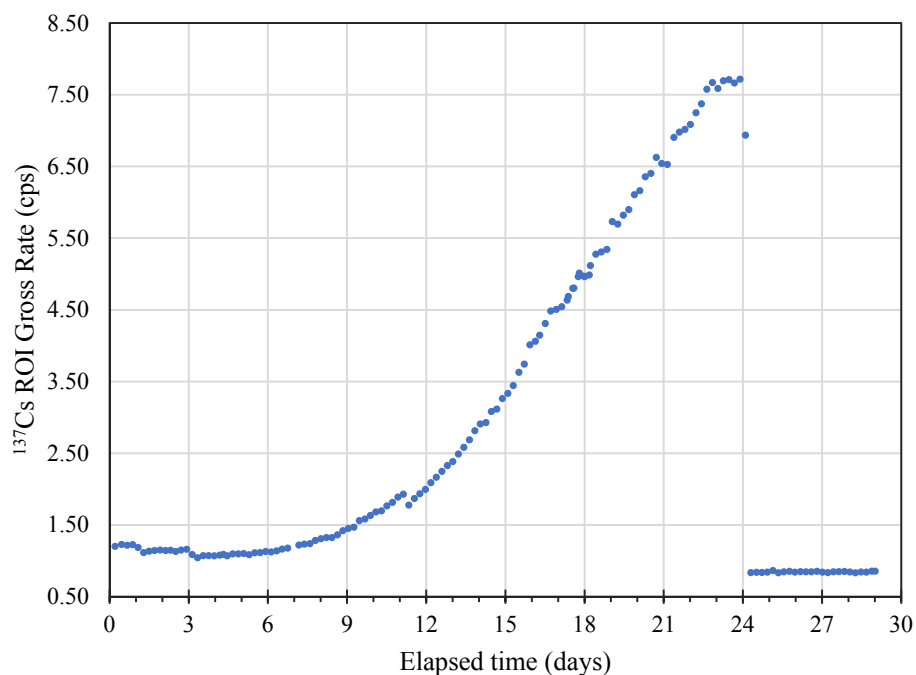


Figure C.6. NaI Flow-through Detector 5-h Gross Count Rates for the ¹³⁷Cs ROI. System background at the conclusion of the ion exchange experiment was lower than at the start of the experiment. A noticeable discontinuity at day 11 was directly tied to radioactive waste movement and removal from the laboratory.

C.4 Conclusion

Overall the in-line detection system(s) proved the efficacy of on-line, real time measurements for tracking ion exchange column performance. The NaI flow-through detector tracked column effluent similar to traditional sampling, but without the need for discrete samples. While data reduction was performed offline in an attempt to minimize performance issues with list-mode acquisition, the analysis and results were easily and reliably performed and displayed real time in the G2K software. An improvement, from a test control perspective, would be to add a calibration feature such that the fraction of Cs in effluent relative to the feed concentration can be determined.

Though the CAEN, list-mode acquisition system availability was disappointing, the acquired data runs demonstrated the potential value overall in using list mode data to track and identify changes in the radioactive effluent. Future CAEN and list-mode acquisition will utilize a dedicated PC and low background detectors if multiple detector(s) are involved. Similarly, while the experiment was not optimized to definitively track ¹³⁷Cs/^{137m}Ba dis-equilibrium directly after ion exchange, it did indicate that a two-detector, online approach could be a viable and useful tool in monitoring ion exchange column performance, whether it be list-mode acquisition and analysis or a more traditional spectrum analysis method.

Pacific Northwest National Laboratory

902 Battelle Boulevard
P.O. Box 999
Richland, WA 99354
1-888-375-PNNL (7665)

www.pnnl.gov